

Addressing on Mechanism of different types of ENSO and related teleconnections and solar influence

Indrani Roy
I.Roy@exeter.ac.uk
College of Engineering, Mathematics and Physical Sciences
University of Exeter
Laver Building
Streatham Campus
North Park Road
Exeter
UK
EX4 4QE

and

R.H. Kriplani
krip@tropmet.res.in
Indian Institute of Tropical Meteorology (IITM)
Pune, India (Retired)
Dr Homi Bhabha Road
Pashan,
Pune-411008, India

Abstract.

A flow chart is presented depicting coupling in ocean-atmosphere system, initiated by solar decadal variability that involves El Niño Southern Oscillation (ENSO). Possible mechanisms for Canonic ENSO, Modoki ENSO and Canonic-Modoki ENSO are proposed considering their relevance to the decadal variation of Hadley, Walker circulation and mid-latitude jets. It also discusses subsequent teleconnections by ENSO on Indian Summer Monsoon (ISM) with a special emphasis on later two decades of the last century. Possible mechanisms relating to a disruption of the usual ENSO-ISM teleconnection for those decades are emphasised; the role of volcanos and the change in the sun- NAO (North Atlantic Oscillation) connection were attended. The regional Hadley circulation, via the NAO in the northern hemisphere and Indian Ocean Dipole in the southern hemisphere, during that period, may have a role in the change in ISM behaviour- which though captured in observation but missed by models. The representation of flow chart helps to improve understanding of various types of ENSO in both temporal as well as spatial scale. The overall study subsequently can benefit the modelling community by not only improved the representation of ENSO in models but also better representation of ISM teleconnection via regional Hadley cell.

1. Introduction.

The El Nino Southern Oscillation (ENSO) is one of the most important modes of variability in the troposphere that influences most parts around the world through teleconnection. It has significant impacts on precipitation at seasonal time scale in several places around the world. Different types of ENSO, based on a spatial pattern of Sea Surface temperature (SST) around Tropical Pacific have been detected and discussed in recent studies. One type is dominated by variability around East Pacific (EP), known as Canonical ENSO or EP type and the other dominated by variability around Central Pacific (CP), known as Modoki or CP type (Trenberth et al., 2002; Larkin and Harrison, 2005; Ashok et al., 2007; Hill et al., 2009; Kug et al. 2009).

Studies suggest there are differences in local and global influences between Canonical and Modoki ENSO (Pacific Rim: Weng *et al.*, 2009; Global: Weng *et al.*, 2007; Ashok *et al.*, 2007; India: Roy and Tedeschi, 2016; Roy et al, 2017; South China Sea: Chang et al., 2008; Australia: Brown et al., 2009; Taschetto and England, 2009, Cai and Cowan, 2009). It indicates the importance of understanding the underlying mechanism of these two types of ENSO to improve prediction skill.

Kao and Yu (2009) in a review compared these two types of ENSO, regarding their evolution and structure. They showed for CP ENSO, atmospheric forcing plays the dominant role while for EP ENSO it is mainly regulated by thermocline shifting (also discussed by Ashok, 2007). Thermocline uplifting for El Nino (EN), while deepening down for La Nina (LN) is related to oceanic Kelvin and Rossby wave movement. That is the reason, the signal of phase reversal is detected only in EP ENSO, but CP ENSO occurs more as epochs or events rather than a cycle. For two types of ENSO, Yu and Kao (2007) indicated the different origin of formation mechanisms. For CP ENSO, its phase transition (barrier, onset etc.) happens in spring and it is phase locked with season; while for EP ENSO, though it is mainly regulated by the thermocline shifting, the phase shift and barrier varies decade to decade. Considering

different times of onset of two types of ENSO, Kao and Yu (2009) indicated it could be related to the timing of mechanisms responsible for triggering particular events. Two mechanisms for extratropical connections for CP ENSO are proposed, Equatorial Ocean Advection Theory (Kug et al. 2009) and Extra-tropical Forcing Theory (Yu et al. 2010, Yu and Kim 2011 and Kao and Yu 2009). Based on the first theory, anomalous SST along the equatorial Pacific is grown by the zonal ocean advection, while the second theory suggests that it is initially excited by forcing from extra-tropics and then developed by the advection from the tropical ocean. Various studies proposed about a decadal connection of ENSO (Henyi and Deng, (2011), McPhaden et al. (2011), Meehl et al. (2008, 2009), Roy, I (2014)). An underlying quasi-decadal variability in the interannual ENSO is noted in several research (Chen et al 2004; Zhang et al., 1997; White et al., 2008; Zhao et al., 2003).

The Sun is the principal source of energy for the climate of the earth, but the level of scientific understanding relating to its effects on the climate is still very low. Though regarding terms of energy output, there is only a 0.1 % variation (Lean and Rind, 2001) between minimum to maximum years of the 11-year cycle, too negligible to influence climate but studies identified significant regional impacts which are often seasonal dependent (Gray et al (2010); Roy and Haigh, (2010); Roy et al (2016)). The signal also fluctuates based on chosen period of reference (Roy and Haigh, (2012)). Decadal signature of solar variability changes is also detected in various atmospheric and oceanic fields. In terms of atmospheric fields it is detected in tropospheric circulations (Hadley Circulation: Haigh et al. (1999, 1996, 2005); Walker Circulation: Meehl et al. (2008, 2009)); Polar Vortex (Kodera, 2002); Mid-latitude Jet (Haigh, 2005; Bronnimann 2006) and Intertropical Convergence Zone (ITCZ) (Lee, et al. 2009). Decadal signature is also distinguished in various oceanic parameters (thermocline: Zhang et al., (2006); North Pacific gyre circulation: Lorenzo et al. (2010) and shallow Meridional Overturning Circulation (MOC) in Pacific: Zhang et al. (2006)).

The ENSO through teleconnection can influence seasonal precipitation in several places around the world, among which Indian Summer Monsoon (ISM) is an important one. Studies have shown that the ENSO strongly modulates the ISM (e.g. Kripalani RH and A Kulkarni 1997; Maity and Kumar, 2006). EN years are usually associated with less rainfall; whereas, LN year experiences more rain. The ISM-ENSO teleconnection was also captured by CMIP5 (Coupled Model Intercomparison Project Phase 5) models matching with observations in parts of Central North East (CNE) region of India around ITCZ (Roy et al (2016)). This is the location where the coupling mechanism of atmosphere and ocean via ENSO through the Walker circulation could be communicated strongly (Gill, 1980). However, ISM and ENSO suggests a weaker correlation during last few decades of the twentieth century and experiences a normal level of rainfall despite EN years (Kumar et al, 1999; Ashok *et al.*, 2001). Ashok et al. (2001) showed that Indian Ocean Dipole (IOD) and ENSO have complementarily affected the ISM during a similar period. They revealed that when the correlation between ENSO and ISM is little, the relationship between IOD and ISM is strong and vice versa. Roy and Collins (2015) using observational data of Sea Level Pressure (SLP) showed that the Southern Oscillation (SO) pattern as captured in the ENSO indicates major changes around Australia in the latter half of the last century. Interestingly, Australia (Darwin), one lobe of Southern Oscillation (SO) is also coincidentally one end of IOD. ISM is also strongly modulated by the North Atlantic Oscillation (NAO) (Liu & Yanai, 2001). The relationship between the temperature of West Eurasia and ISM is stronger, over the same period the relationship between the ISM and ENSO has weakened (Chang et al., 2001). According to them, as the ENSO ISM teleconnection became weaker, the possibility for the NAO to influence the ISM through the above mechanism has enhanced. The connection between IOD, ISM and NAO are in favour of a linkage that involves regional Hadley circulation and ITCZ and follows mechanism of Gill (1980). According to that mechanism the ISM represents a large-scale source of heat around the CNE region and following the linear theory it could be related to both Walker and regional Hadley cell.

The regional monsoon–ENSO relationship is shown having common changing points around the 1970s. There was an enhancement of the relations for the western North Pacific, North American, Northern African, and South American summer monsoons, with a recovery in the late 1990s. Interestingly, for the ISM, it weakened over the same period (Yim et al. 2013). Such a changing pattern of monsoon under global warming scenario is also discussed by. Huang, P. et al. (2013) in a recent study. A decreasing trend in precipitation around India detected in observations (Ramanathan et al. 2005, Chung et al. 2006, Goswami (2006)) contradicts the proposed hypothesis based on thermodynamic scaling arguments (Held and Soden (2006)). The direction of anomalous change in circulation, both the Walker and Hadley circulation and their relative strength around the Indian subcontinent, mainly in the CNE region, under climate change scenario, needs additional attention (Bollasina, 2011). Interestingly, observation indicates that the nature of ENSO also changed over the similar period; ENSO Modoki became more persistent and frequent since the 1970s (Ashok and Yamagata, (2009); Yeh et al. (2009)). Research suggests that the increase of ENSO Modoki during latter decades of the last century could also be due to parts of decadal nature variability (McPhaden 2011).

This study focuses on some of those important issues as mentioned. This paper is structured as follows. Section 2 describes Methodology and Data and Results are discussed in section 3. The initial part of section 3 focuses on formulating a Flow Chart and proposing mechanisms for various types of ENSO. The second part covers the so called ‘Climate change period’ and its relevance with changing pattern of ISM. It discusses spatial pattern as well as the temporal behaviour of various climate modes and indices. Section 4 mentions about Conclusions. Overall, this study will discuss various influences on different types of ENSO originated especially via the solar cycle variability. The related teleconnections with the ISM will also be attended giving special emphasis on the so called ‘climate change’ period.

2. Methodology and Data.

The first part of this study covers a schematic representation that considers several highly cited research and formulates a flow chart, providing a holistic representation of various processes.

In the later part, the method of Multiple Linear Regression analysis with AR (1) noise model is used. In this methodology, with the components of variability, noise coefficients are calculated simultaneously. It is done in a way that the residual is consistent with a red noise model of order one and thus it is possible to minimise noise to be interpreted as a signature. Finally, measures of the significant levels are calculated, using Student's t-test. This model is developed by Myles Allen, The University of Oxford and this methodology was widely used in various climate studies (Gray et al 2010). Of late, Roy and Haigh (2010, 2011, 2012), Roy (2014), and Roy et al. (2016) also applied this technique to analyse various climate data.

Variables and climate indices employed in the regression are Sea Level Pressure (SLP), monthly Sun Spot Number (SSN), Niño3.4 (to represent ENSO), Stratospheric Aerosol Optical Depth (AOD), (indicative of volcanic eruptions) and longer term trends. The ENSO data used here are anomaly value and all the data are normalised before an analysis. For SLP, the in-filled HadSLP2 dataset, which covers the whole globe (Allan et al. (2006)) and available as monthly means from 1850 to 2004 are used. It can also be found from <http://www.metoffice.gov.uk/hadobs/hadslp2>. Error estimates are mentioned for HadSLP2 (Unlike HadSLP1), to have ideas about the regions of little confidence. It has been updated upto 2012 using HadSLP2r_lowvar data (<http://www.metoffice.gov.uk/hadobs/hadslp2/data/download.html>). It is a version of HadSLP2r and consistent with HadSLP2. The global monthly HadSLP2r data that covers 2005 to 2012, is the NCEP-NCAR Reanalysis data (Kistler et al., 2001), which is adjusted as its average for period 1961–1990 matches with HadSLP2. In the recent version of HadSLP2r_lowvardata, the deficiency concerning the difference in invariance between HadSLP2 and HadSLP2r is adjusted. Monthly Sun Spot Number (SSN) is

used to represent solar cyclic variability and obtained from ftp://ftp.ngdc.noaa.gov/STP/SOLAR_DATA/SUNSPOT_NUMBERS/INTERNATIONAL/monthly/MONTHLY.PLT. For the ENSO, Niño 3.4 index, obtained from Kaplan et al. [1998] is used which is available since 1856 and can also be found at <http://climexp.knmi.nl>. In the regression, AOD has been used to represent volcanic eruptions and collected from Sato et al. (1993) and available from https://data.giss.nasa.gov/modelforce/strataer/tau_line.txt (up to 1999). It is then extended up to 2005 with near zero value. It can also be obtained from KNMI Climate Explorer (<http://climexp.knmi.nl>). Longer term trend is a rising linear line that represents increasing anthropogenic influence.

For trend analysis, various indices we used are the NAO, Southern Annular Mode (SAM), IOD, Niño temperatures (12 and 3.4), EP and CP ENSO, SLP Darwin and Tahiti and regional ISM precipitation. For NAO, DJF value is considered and for the rest, a seasonal value of JJA is used. This is because studies (Liu & Yanai, 2001, Xavier, et al. 2007) suggested winter NAO and Eurasian temperature has impacts on ISM (JJA). The discriminates for different trend period is used, e.g., 1970, 1976 or 1957, which are based on following justifications: the 1970s is an abrupt drop in SSTs (Thompson et al. 2010); 1976 is the well-known Pacific regime shift (Miller, 1994); 1957 could be justified instrumentally as it is termed as International Geophysical Year (IGY) and from that period many other studies started. Other reasons for justification are also mentioned in the text.

The monthly EP and CP indices are calculated (Yu and Kim 2010; Kao and Yu 2009) from Extended Reconstructed Sea Surface Temperature (ERSST) dataset (Smith and Reynolds, 2003) that used 1971-2000 climatology and available from 1948 to 2014. The relevant web links for EP and CP ENSO data are:

http://www.ess.uci.edu/~yu/2OSC/monthly_CP_index_1948_2014.txt and

http://www.ess.uci.edu/~yu/2OSC/monthly_EP_index_1948_2014.txt

Yu and Kim (2010) and Kao and Yu (2009) used a regression-EOF technique to identify the EP and CP types of ENSO and briefly discussed as follows. They considered the Nino1+2 index (80W-90W; 0-10S) as an estimate to eliminate the effect of the EP ENSO to that from CP ENSO. For CP ENSO, the anomalies in SST are regressed with the Nino1+2 SST index first removed from the total anomalies. Then an EOF analysis was applied to obtain a spatial pattern of the CP ENSO. Similarly, for EP ENSO, they subtracted the SST anomalies regressed with the Nino4 index from the total anomalies in SST, before applying the EOF technique to identify the leading pattern of the EP ENSO.

The NAO index from Climate Research Unit (CRU), University of East Anglia is used which is available since 1823. It is developed by Jones et al., (1997) that considered instrumental pressure observations from Gibraltar and south-west Iceland. It is also available from http://www.cru.uea.ac.uk/~timo/projpages/nao_update.htm. The other indices as mentioned are all available from <http://climexp.knmi.nl>. The ISM data is also present in the Indian Institute of Tropical Meteorology (IITM). (Link: <ftp://www.tropmet.res.in/pub/data/rain/iitm-imr-readme.txt>). ISM rainfall data are used for three arbitrary regions, Central North East India (covering five subdivisions), all India rainfall (thirty sub-divisions) and Peninsular rainfall (includes six subdivisions). The details about subdivisions and areas are well documented in <http://climexp.knmi.nl>. For IOD, it is calculated as the difference of SST (°C) from NOAA ERSST (Smith and Reynolds, 2004), version 4 (in situ only) from two regions. It is the SST of a region (39° to 81°E, 15°S to 15°N) to that from the region (89° to 101°E, 11°S to 1°N).

To detect significant testing in the trend, Mann-Kendall test (Kendall, M. G. (1970), Myles Hollander and Douglas A. Wolfe (1999)) is used.

3. Results.

3.1. Formulation of Flow Chart - Proposed Mechanism:

Here, I develop a flowchart (Fig. 1), depicting a consolidated overview of ocean-atmosphere coupling, supported by highly cited popular research. Initiated by solar decadal variability how

coupling in atmosphere-ocean is taking place is presented. The major climate variabilities; viz. ENSO and Solar are shown with oval outlines; whereas, the major circulations (Walker, Hadley Ferrel cell), responsible for modulating the influence of major variabilities are shown by non-rectangular parallelograms. Pathways of the signature are shown by labels that start from 'A', which is initiated by solar variability and the direction of behaviour change during the steps by '-' (for decrease) and '+' (for increase). The flow chart depicts the role of the sun and how the atmosphere and ocean coupling regulates the formation of various types of ENSO, viz. the Canonic ENSO, Modoki ENSO and Canonic-Modoki ENSO. The related teleconnection with ISM is also presented. Dash dotted lines mark the pathways those are affected by so called 'climate change' signal. A similar flow chart was also formulated in the study of Roy, I (2014) that however did not consider different forms of ENSO.

Two fundamentally different routes for a solar influence on the troposphere have been proposed: one is the 'Bottom-Up' mechanism (Meehl et al (2008, 2009)) and the other the 'Top-Down' mechanism (Haigh and coworkers (1996, 2005, 2006); Kodera and Kuroda (2002); Baldwin and Dunkerton (2001)). In the 'Bottom-Up' pathway, the Sun can directly affect SST without stratospheric feedback; whereas, the 'Top-Down' influence of the sun is originated through the stratosphere. Roy, I. (2014) elaborately documented more detailed discussions. Frame and Gray (2009) showed using the observation that there is a cooling (warming) in the lower equatorial stratosphere during solar minimum (maximum) years (A, Fig. 1). Haigh and coworkers (Haigh et al, 2006; Haigh, 1996; Haigh et al, 2005) noted, an impact on tropospheric mean meridional circulation, characterising a weakening and expansion of the tropical Hadley cells, along with a shift of the Ferrel cells pole ward (A, B, C, Fig. 1). It also leads to coherent changes in the width and latitudinal location of the mid-latitude jet stream (D). Observational work of Brönnimann et al. (2006), also supports such findings. A possible mechanism was proposed by Kodera and Kuroda, (2002), whereby the solar influence can change equatorial stratospheric region through changes in the meridional circulation, that also involve polar vortex (E). According to them, the sun can influence the path of upward

propagating planetary waves because the sun's heating anomalies can alter the strength of polar upper stratospheric jet. These waves, weaken the Brewer-Dobson Circulation (BDC) via depositing their zonal momentum on the poleward side of the jet in solar maximum years and subsequently warm the tropical lower stratosphere. Solar decadal variability regulates the strength of polar vortex by normal thermal wind balance relationship as labelled here by F. Baldwin et al. (2001) showed perturbations in the polar vortex, are related to polar annular modes (G). They discussed a dynamical mechanism that might communicate stratospheric circulation anomalies downward to the tropospheric surface via polar modes. Meehl et al. (2008, 2009) presented a mechanism related to sea-air-radiative coupling involving the sun. They discussed that the spatial asymmetries of solar forcing, induced by cloud distributions, can cause greater evaporation in the subtropics. It consequently causes more moisture transport and intensification of the tropical convergence zone and strengthens the trade winds around tropical Pacific (H, I).

Through normal ENSO mechanism, involving deepening of the thermocline (J, K), it subsequently intensifies Walker circulation (L). Shifting of the thermocline is then regulated by Oceanic Rossby and Kelvin waves which control the inter-annual nature of ENSO. It is consistent with studies that detected decadal signature in thermocline (Zhang et al., 2006). Some wind triggering mechanism around tropical Pacific responsible for initiation of Kelvin and Rossby wave is needed, though source being still unclear (Vecchi and Soden, 2007). The proposed flowchart suggests the sun could be a possible candidate. Roy and Haigh (2010) also captured similar decadal signature in trade wind (I) in an observational analysis. The proposed pathway (K) matches to that with EP ENSO. Ashok et al. (2007), Kao and Yu, (2009) suggested that thermocline shifting is known to be the main driver for EP ENSO. A signature of phase reversal is also identified in EP type of ENSO with its major phase transition and the barrier was found to change decade to decade (Kao and Yu (2009)).

The weakening of Ferrel Cell is associated with weakening of Aleutian Low (AL). Christoforou and Hameed (1997) showed that solar variability causes shifting the location of AL alongside creating significant differences in intensity (M). Observational analysis by Roy and Haigh (2010) and Van Loon et al (2007) is also consistent with such findings. Decadal variability around AL could be responsible for North Pacific warming (N). Such decadal signature around mid-latitude was captured in observation by Frame and Gray (2009), Haigh (2003). North Pacific Gyre circulation which is wind driven is also affected through AL. Decadal signature in North Pacific Gyre was observed by (Lorenzo et al 2010).

Warming around North Pacific is connected to the shallow conveyor belt of the ocean which has a rising branch around North Pacific near AL. That shallow ocean conveyor belt is flowing through tropical Pacific and links tropics to North Pacific via ocean pathway (Q). That tropical Pacific part can sometimes be termed as shallow Meridional Ocean circulation (MOC) in the Pacific. It characterizes the equatorward convergence of the pycnocline volume transport across 9°S and 9°N. Using historical hydrographic data, Zhang et al. (2006) observed decadal variability in the Pacific shallow MOC. Ocean subduction pathways could also act as links between North Pacific to tropics mass exchanges.

The strength of annular mode has the potential to change the intensity/ location of tropospheric jets via usual mechanism and can influence North Pacific (O, P) (double-ended arrow show the two-way interactions). It can subsequently modulate mid-latitude ocean gyre through wind stress. The decadal signal around North Pacific could be transported to tropical Pacific via ocean pathway (P, Q, R) to trigger Modoki ENSO feature (R). Lorenzo et al. (2010) showed decadal variations in the North Pacific gyre circulation are characterized by a pattern of SST anomalies resembling the CP type ENSO. Sullivan et al, (2016) discussed that CP ENSO shows a dominant spectral peak at a decadal time scale, which in an interannual period possess a comparatively weaker variance. They showed there is a significant reduction in the frequency of the CP ENSO in observation and also in CMIP5 simulations of historical, preindustrial, and future scenario if that decadal component is removed.

Apart from oceanic connections, changes in the mid-latitude jets and Aleutian low can also directly impact CP ENSO, through dynamic variability of the Hadley circulation. All such discussions are consistent with proposed mechanism of CP ENSO. For CP ENSO, as seen in the flow chart atmospheric forcing plays the dominant role as proposed by (Kao and Yu (2009)) and it has extratropical connections. Aleutian Low could play one dominant role and shown by S. Two mechanisms for CP ENSO for extratropical connections were discussed earlier e.g., Equatorial Ocean Advection Theory (Kug et al. 2009) and Extratropical Forcing Theory (Yu and Kim 2011, Yu et al. 2010, Kao and Yu 2009) which are in agreement with those proposed pathways. The first theory, suggests anomalous SST along the equatorial Pacific is grown by the zonal ocean advection, while the second indicates it is initially excited by extra-tropical forcing and then developed by the advection from the tropical ocean. It is also consistent with the observation that the CP ENSO occurs more as events or epochs than as a cycle as noted for EP type (Kao and Yu (2009)). The phase locking of CP ENSO with the season, having phase transition in spring (Yu and Kao (2009)) also supports a solar connection. Mantua and Hare (2002) indicated that Pacific in the mid-latitude and tropics is connected via ocean pathway. The pathway that establishes the linkage between tropics (via thermocline shift) and extratropics as shown by T governs ENSO Canonical and Modoki (CM) combined feature. Overall, the flow chart is consistent with studies those detected an underlying quasi-decadal variability in the interannual ENSO (White and Liu, 2008; Zhang et al., 1997; Zhao et al., 2003; Chen et al. 2004).

Now I present discussions that also involve ISM. The ISM represents a large-scale heat source on the equator located at a mean position of about 20-30N (around ITCZ) covering the region of CNE. Following the linear theory, the response to such a heat source suggests that it will be related to Walker circulation as well as regional Hadley circulation (Gill 1980). The Walker cell is related to equatorial heat sources and is regulated remotely by tropical Pacific whereas, the local Hadley cell shows a direct response to the off-equatorial heat source. The location and strength of the monsoon heat source can also impact Walker and regional Hadley cell.

Lee, Shindell et al (2009) studied decadal variability on ITCZ and found during active solar periods there is an enhancement of the strength. Pathways V and W indicate about such relationship with ISM and tropical circulations involving ITCZ (direction of change is not considered here).

The influence of ENSO in reverse direction is also noted in various studies. The ENSO through Brewer-Dobson circulation can also influence polar vortex (U) and subsequently to extratropics in an inverse pathway and shown in the flow chart. During winter, Camp and Tung (2007), showed warm-ENSO years are significantly warmer at the Northern Hemisphere polar and mid-latitudes in the stratosphere than the cold-ENSO years. Taguchi and Hartmann (2006) and Sassi et al. (2004), using a GCM showed that the warming difference between La Niña and El Niño years is statistically significant. They showed in the El Niño winters, Stratospheric Sudden Warming (SSW) are twice as likely to occur than La Niña years. It indicates a possible connection between the ENSO and polar stratosphere. The ENSO can also influence tropospheric jets and polar annular modes were shown by Carvalho et al. (2005), Haigh and Roscoe (2006) (O, P in reverse direction).

Observations, as well as model simulations, suggested that it could be two way interactions and both types of El Niño also have potential to modulate the extra-tropics (even true for EP ENSO). CP ENSO influence is mainly seen around Southern Hemisphere (SH), though EP in the NH. For CP ENSO, the variations in wind etc. are mainly localised around the central Pacific (Kao and Yu (2009)). It enhances convective activity in the South Pacific Convergence Zone in austral spring and affects Antarctic surface temperatures and sea ice concentrations (Song et al. 2011, Schneider et al. 2012). The mechanism how EP ENSO could influence extra-tropics of NH is also discussed (Randel et al. (2009), Manzini et al. (2006) and Garcia-Herrera et al. (2006)). As EP ENSO is mainly regulated by thermocline shifting and shows basin wide variation of several features (Kao and Yu (2009); Ashok, (2007)), it possesses the potential to perturb planetary scale Rossby waves, which are mainly generated in the NH due

to ocean land contrast. The enhanced planetary wave driving leads to a weakening of the Arctic vortex and warm the polar stratosphere in boreal winter. It subsequently, deepens the north Pacific AL. In the absence of land ocean contrast, planetary wave activity in the SH plays a nominal role and hence EP ENSO does not impact the extra-tropics in SH (Hurwitz et al. 2011).

McPhaden and Zhang (2004), Vecchi and Soden (2007), Held and Soden (2006) suggested there is a substantial, decrease in the strength of both Walker and Hadley circulation since the 1950s as marked here by X and Y. It is likely to be reflected simultaneously in ISM as well as ENSO (Z). Roy and Haigh (2012) showed over the similar period, decadal signature around trade wind as demonstrated by J is missing, probably due to change in mean state. It indicates a weakening of EP ENSO-related mechanism that involves thermocline. A recent study suggests, ENSO Modoki has become more frequent and persistent than Canonic ENSO since the later period of last century (Yeh et al. (2009); Ashok and Yamagata, (2009)). The change in ISM over a similar period is also well documented in various studies (Ashrit et al. 2001, Ashok et al. 2001). The climate change signal via X, Y, Z subsequently affects ISM, using pathways V and W.

In the flowchart (Fig. 1), there could be various other pathways for e.g. including major variability QBO (shown in Roy, I (2014)); but for clarity, we avoided enough complexities. Also, for presenting climate change signals (shown by the dotted dash line) we avoided complicated pathways. More related discussions on so called 'climate change' are covered in the subsequent sections.

Labels agreeing on various pathways/ studies as discussed here (Fig. 1) are listed underneath to improve clarity:

A: Haigh (2003), Frame and Gray (2009),

A, B, C, D: Haigh et al. (2005), Brönnimann et al. (2006), Haigh (1996, 1999)

E: Koderä and Kuroda (2002)

F: Usual mechanism following thermal wind balance.

G: Baldwin and Dunkerton (2001).

H, I: Meehl et al. (2008, 2009).

I: Roy and Haigh (2010)

J, K, L: Normal ENSO (inter-annual) mechanism.

K: Kao and Yu (2009); Ashok et al. (2007); Zhang et al. (2006)

M: Christoforou et al. (1997), Roy and Haigh (2010), van Loon et al. (2007)

N, P: Haigh (2003), Frame and Gray (2009).

O, P: Carvalho et al. (2005), Haigh and Roscoe (2006)

O, P, Q, N: Usual ocean-atmosphere interaction involving wind stress.

R: Kao and Yu (2009); Yu and Kao (2009)

S: Kao and Yu (2009)

T: Mantu and Hare (2007)

U: Camp and Tung (2007); Sassi et al. (2004); Taguchi and Hartmann (2006)

V, W: Gill (1980).

X, Y: Held and Soden (2006), Vecchi and Soden (2007), McPhaden and Zhang, (2004).

Z: Ashok and Yamagata (2009), Yeh et al. (2009)

Table 1 indicates how each link is explained by a mechanism, evidenced by observation, or only be viewed as a hypothesis at this stage. Some pathways are also kept as hypothesis stage partly because those are based on model experiments or observation, but still, needs improvements

3.2. ISM and Climate change

3.2.1. Results of Regression:

Signature due to the Sun:

ENSO Modoki has become more persistent and frequent than Canonic ENSO since the 1970s (Yeh et al. (2009), Ashok and Yamagata, (2009)). Three separate MLR analyses on SLP data (DJF) are carried: one for the whole period (Fig. 2a); other two before and after 1970 (Fig. 2b and Fig. 2c respectively). Strong signal around AL is noticed in all plots. Interestingly, such strong solar signature in SLP around AL during northern winter is robust and found insensitive to various methodologies and time periods (van Loon et al, 2007, Hameed et al, 1997). Roy et al. (2016) did seasonal analysis and showed that solar signal around AL is only present during DJF. That signal is seen to be reduced in Fig. 2c to that from Fig. 2b.

Signature of the sun around central tropical Pacific is also different in those two periods (Fig. 2b and 2c). A small but significant decadal signature is present in SLP before 1970 (Fig. 2b) that could play a role in triggering trade wind. Fig. 2a for the whole period also indicates significant signal though weaker in magnitude than Fig. 2b. Such solar signal on trade wind could be responsible for initiating ENSO through an indirect dynamical coupling (discussed in details by Roy, (2014)). Instigating Oceanic Rossby and Kelvin waves it has a potential in shifting thermocline and subsequently trigger EP ENSO. Such signature of decadal nature could be present in EP ENSO in addition to its interannual variability, regulated by Oceanic

Kelvin and Rossby wave movements. Decadal signature on thermocline is noted in various studies (Zhang et al., (2006). It is also consistent with the earlier discussion, (Yu and Kao, 2009) who indicated that for EP type, the phase transition and barrier change decade to decade and it is mainly regulated by thermocline shifting. That solar signature in trade wind is absent since 1971 (Fig. 2c) and could be one possible cause for dominance of CP ENSO over EP (Ashok and Yamagata, (2009); Yeh et al. (2009)).

Positive NAO pattern for the sun is clearly distinguished in the later period (Fig. 2c), which is different during an earlier period (Fig. 2b). Perturbations around North Atlantic was found as a precursor of CP ENSO (Ham et al., 2013a, 2013b) and the mechanism involves atmospheric Rossby wave. Positive NAO via triggering Rossby wave around mid-latitudes could influence north Pacific (AL is likely to be modulated) and subsequently has the potential to initiate CP ENSO through the atmospheric and oceanic bridge (for e.g., Extra-tropical Forcing Theory (Yu et al. 2010, Yu and Kim 2011 and Kao and Yu 2009)). It was noted that the change in CP ENSO in recent decades could also partly be due to decadal nature variability (McPhaden 2011). Sullivan et al, (2016) discussed that CP ENSO shows a dominant spectral peak at a decadal time scale, which in an inter-annual period possess a comparatively weaker variance. Over last few decades, that decadal variations have an important contribution to the occurrence of CP ENSO (Sullivan et al. 2016). Regression results suggest the Sun-NAO changing behaviour (Fig. 2c) could be a responsible factor.

Regional Hadley circulation also plays a role. Bjerknes (1966) showed that the major warming along the central and equatorial Pacific during boreal winter is often accompanied by an anomalous strength of the mid-latitude westerlies. There is a two-sided interaction. The anomalously great heat from the equatorial ocean to the rising branch of the Hadley circulation would strengthen the cell. It will generate above normal flux of angular momentum to the westerly winds around mid-latitude belt. Thus, warming in the tropical Pacific can strengthen the mid-latitude westerly jets during boreal winter and subsequently can favour positive phase

of the NAO. Following the similar mechanism, positive phase of the NAO can also favour positive phase of CP ENSO.

However, it is not only the sun that has modulated CP ENSO via NAO, volcano during later two decades of the last century, could also be responsible.

Signature due to Volcano:

Fig. 3 shows the result due to volcano over the period 1856 to 2012. Positive NAO pattern is clearly distinguished for active volcanos as also noticed in other studies (Roy et al. (2016) among others. Two major volcanos erupted during 1981 and 1992, which were strongest ever in the record of past 150 years. Contrary to the earlier eruptions, those two even coincided with active phases of high solar cycles. It is indicated that the relationship between NAO (DJF) and ISM has become stronger, over about the same period the relationship between ISM and ENSO has weakened (Chang et al, 2001). The result of regression suggests two explosive volcanos, via modulating the NAO, could be one responsible factor for such a change in ISM. Due to the absence of major volcanos in current decades, such association involving NAO weakened, suggesting it could be one possible cause that correlation between ENSO and ISM is reverted since the late 1990s (Yim et al (2013)). It is also noted that ISM precipitation has likely increased over the last decade, after reversing the drying trend that happened from the mid of the 1970s to mid of 1990s (IPCC, 2013).

The influence of explosive volcanos on ENSO phase was discussed in various observational (Adams et al. (2003), Emile-Geay J.,(2008)) as well as modelling experiments (Stenchikov et al. (2009), Ohba et al., (2013)), which univocally suggested a significantly rise in the likelihood of El Niño events. Ohba et al., [2013] using a Model for Interdisciplinary Research on Climate (MIROC5) suggested about excitation of the anomalous Pacific westerly for explosive volcanos which subsequently causes an increase in the probability of El Niño. Their model result indicates that explosive volcanos during El Niño phase contribute to the

duration of El Niño, whereas the same during La Niña shortens its period counteracting to its duration. Using Geophysical Fluid Dynamics Laboratory (GFDL) CM2.1 model a similar response is also noticed by Stenchikov et al. (2009). They discussed that such effect on El Niño arises due to the amplification by the air-sea coupled feedback. Without major volcanos, ENSO cycle is likely to show equal tendencies for warm as well as cold phase and also favours the recovery of that drying trend (IPCC, 2013), following usual ENSO-ISM anti-correlation.

In the subsequent section, additional attention will be on the NAO and CP ENSO.

3.2.2. Time series Analysis

The ISM–ENSO relationship is found to have common changing points in the 1970s. Though weakened since then showed a recovery in the late 1990s (Yim et al (2013)). An analysis based on time series of various modes of climate variability is performed with particular emphasis on the period 1976-1996, to investigate such connection further. It covers two full solar cycles, (cycle number 21 and 22) starting from one solar minimum (1976) and ending with another solar minimum (1996). The consecutive solar peak years are 1979 and 1989 with one minimum in between (the year 1986). During that period, two major volcanos erupted during active years of stronger solar cycles. A study suggested separating the period 1979–1997 is important to understand some climate features better (Roy, I, 2016). Such observation was strengthened by very recent studies (Polvani et al. 2017, Oliva et al. 2017) and indicated that it is indeed true.

Figure 4 shows normalised time series of various seasonal modes of climate variability those might be related to different types of ENSO (EP or CP) and also regional ISM rainfall, as shown by their subtitles. The top panel (Fig. 4(i)) is during period 1871-2011 and the bottom panel (Fig. 4(ii)) for 1957-2012. For NAO, DJF value is considered and for the rest, seasonal value of JJA is used. Five-year running mean of each series is marked by red in each panel.

A trend line is plotted during 1976-1996 for all series of bottom panel and shown by a blue dashed line. The period of 1976-1996 is demarcated by black dash lines in Fig. 4(ii).

Noting Fig. 4(i), it can be stated that there is no apparent clear trend in any of those time series for the whole of the record. We could not identify decreasing trend of ISM (IPCC, 2013) in the arbitrary chosen regional ISM rainfall. It could be due to a precise location of CNE India, covering the ITCZ that only showed the decreasing trend in a spatial pattern (Bollasina et al. (2011) and Goswami (2006)). The time series of regional ISM considered here might have other opposing local influences. Interestingly, when the focus is around 1976-1996, a clear trend is noticed for SLP Darwin and IOD (Fig. 4(i)). Hence, we analyse it further in Fig 4(ii) considering shorter record (1957-2012) demarcating that 20 years period.

Time series of few other parameters were presented which are thought might be linked to those two parameters (IOD and SLP Darwin). SLP around Darwin was chosen because an increase in SLP here strengthens ITCZ. The rise in pressure gradient between Darwin and ITCZ enhances the flow of moist rich ocean air. More air from the Indian Ocean converge towards the land region of India and increase rainfall. CP and EP ENSO series are constructed since 1948 ((Kao and Yu 2009; Yu and Kim 2010) and we presented those in Fig. 4(ii) as those are more relevant to our discussion. Among those parameters, there is a clear rising trend for CP ENSO, NAO, SLP Darwin with a decreasing trend for EP ENSO and IOD during 1976-1996. All the parameters suggest nominal, an insignificant rising trend over the whole period (1957-2012).

CP ENSO indicated a clear upward trend (11 % per decade, increased significantly; for whole period it is 1.4%) which is consistent with the observation that ENSO Modoki became more familiar since the 1970s up to late 1990s. It is in agreement with rising trend of NAO (+15%

per decade, whole 1.3%). The connection between CP ENSO and NAO, both suggest increasing trend, agrees with the proposed mechanism of Bjerknes (Bjerknes (1966) as discussed earlier) and also the mechanism involving extratropical Rossby waves (Ham et al., 2013a, 2013b). Annular modes in NH have exhibited pronounced trends toward high-index polarity also documented by Hurrell (1995) and Thompson et al. (2000). The EP ENSO, on the other hand, shows a decreasing trend (-11% per decade, but not significant; whole 0.4 %).

The influence of ENSO Modoki on Southern Hemisphere storm track activity during JJASO (June– July–August–September–October) was discussed by Ashok et al. (2009). It showed El Niño Modoki introduces a blocking over central eastern Australia which subsequently suppresses the regional storm track activity. Following an increase of ENSO Modoki since the 1970s, it would undoubtedly suggest a rise in SLP around Darwin, Australia as also noticed in Fig. 4 (ii) (trend = +15% per decade, whole 3.8%). Roy and Collins (2015) also noticed that SLP of Darwin is strongly influenced during later periods. Thus, ENSO Modoki through blocking over Australia, one end of IOD, can have potential to influence IOD and subsequently ISM (trend of IOD = -20% per decade, significant at 95% level; whole .3%). Following the definition of IOD as used here, the direction of the trend for IOD and SLP of Darwin suggests a consistent result. There could be an argument that if SLP of Darwin has the potential to influence ISM, then a clear trend observed there should also be seen in ISM rainfall time series. But it is not the case because ISM is not only regulated by moisture convergence from the Indian Ocean alone. Large-scale circulation features like Walker circulations and Regional Hadley circulation also play dominant roles, apart from other local influences. All those forcing acts in a complex nonlinear manner to produce the actual response on ISM and hence no clear trend is noticed.

The response relating to Hadley cell and upper air midlatitude westerlies can be explained by the mechanism proposed by Bjerknes (Bjerknes (1966)) and is expected to be strongest in the winter hemisphere due to greater baroclinicity. Hence, it would also be captured in the

strength of SAM. The ENSO Modoki which is dominant since the 1970s, though suppresses rainfall over India, enhances over North and South America. Rainfall in central Argentina is also increased owing to the strengthened upper air westerlies (Ashok et al. (2009)). Amita et al. (2015) studied trends in SAM during 1949-2013 and found that the data from post-1982 does not show significant long-term trends. It is because of opposing nature of the strength of westerlies around the whole of the mid-latitude to that from Darwin of Australia. That could be one responsible factor to suggest null results for SAM trend when considered in a zonal sense. It is consistent with the current analysis as we also could not identify a significant rising trend for SAM (trend is only -8% per decade and insignificant) during that period (the whole trend is +2%). In the subsequent section, there will be more focus on the NAO, IOD and SLP at Darwin of Australia.

3.2.3. Observation and CMIP5 model results:

From the last 100 years of Darwin's mean sea-level pressure record of last century, Trenberth and Hoar (1996) reported that the Darwin pressure has tended to be above its long-term normal since 1977 and suggested it might be due to the influence of the enhanced greenhouse effect on the climate system. However, contrary to that, Harrison and Larkin (1997) indicated about the impact of natural variability on the tropical Pacific.

Mean surface pressure (which is similar to SLP) is plotted in Fig.5 during June-August with a special focus on Indian Ocean region. Spatial pattern using ensemble mean of AR5 CMIP5 subset model (bottom) indicates a reduction of pressure during 1976-1996 w.r.t. reference period 1997-2016 (left) around Darwin of Australia, and regions of IOD. Consistent with longer term trend similar locations suggest an increase in pressure when the reference period is switched to 1956-1975 (Right). Interestingly, respective figures using observational data of HadSLP2r (top) deviates to that from model results. Places around Darwin of Australia show a rise in pressure for both the cases of observation. Moreover parts of the Indian subcontinent,

and regions of east Africa, where the influence of IOD is felt, also show an enhancement in both the cases. Such analyses indicate, the influence of surface pressure around Darwin of Australia and regions of IOD show some special characteristics (a rise) during 1976-1996, which is different to that from the signal of a longer trend. Model results fail to detect it but capture well the longer term trend instead. In left, surface pressure around Darwin of Australia is shown by blue in the model; which is brown in observation. Those signatures are not only reverse in nature but in both cases even higher than one standard deviation of natural variability (shown without hatching).

Two arbitrarily chosen CMIP5 models (CanESM2 and IPSL-CM5A-LR) are also tested for Mean surface pressure (June-Aug) in Fig. S1. There is no consistency noticed in these two models. In Indian Ocean region. CanESM2 is dominated by blue in both the anomaly period (earlier or recent); whereas IPSL-CM5A-LR suggests red.

Fig. 6 is same as Fig. 5 respectively but depicts the North Atlantic region for DJF season. The places around Icelandic Low and Azore High in models (bottom) clearly detect longer term trend (opposite signature in two plots) for surface pressure. However, models cannot distinguish any patterns of NAO and signals are similar in those two places on the right as well as the left plot. The observational data from HadSLP2r suggests differently to that from models in terms of NAO pattern. Positive NAO feature is distinct in the right panel, which even exceeds the range of natural variability around the Icelandic Low and Azore High. Unlike model results, opposite signal is also noticed in those two places, in the left panel; though deviation lies within the range of natural variability. Moreover, negative NAO pattern is not very distinct in that left plot. Interestingly, observation suggests the opposite to that from Model in both cases around Icelandic low.

All these studies suggest local N-S Hadley circulation, as manifest as NAO in the NH and IOD in SH may have played a role in modulating ISM in later decades of last century (1976-1996).

Such features though captured in observation but missed by models. Observation suggests complex interplay among NAO and IOD on ISM via Hadley circulation has potential to modulate ISM, which is not captured by models. Roy and Tedeschi (2016) showed almost all CMIP5 models poorly represent the observed influence of meridional circulation on ISM; deviates largely from observation, but surprisingly consistent among each other. Apart from the influence of E-W Walker circulation on ISM, the contributions from N-S Hadley cell needs additional attention; which were shown could be more relevant during later two decades of the last century.

Turner and Annamalai, (2012) used CMIP3 model analyses to examine/compare ISM precipitation with observation and elaborately discussed various issues why models failed to match observations. They, however, noted the correlation between ISM and ENSO wanes and waxes to a certain degree in models which are decadal in nature. But, in the phase among the realizations, there is little consistency in models that points towards a lack of predictability of the decadal modulation of the ENSO-monsoon connection (Turner and Annamalai, 2012). They indicated further understanding and model improvements are necessary to improve ISM prediction skill. Using model, Cash et al. (2017) discussed that for observed fluctuations in the NINO-ISM correlation, sampling variability can also be a responsible factor. In terms of mechanisms relating to disagreement among observation and model results, various studies addressed it from various angles, those include aerosol-based changes (e.g. Bollasina et al. 2011); circulation-based changes (e.g. Annamalai et al. 2012); sea-surface temperatures in the Indo-Pacific (e.g. Roxy et al. 2015)). Systematic errors are also there in the ENSO and ISM simulations and all these caveats should be considered while interpreting ISM-ENSO diagnostics and the response of ISM in global warming scenario (Annamalai et al. 2007).

4. Discussion.

A flow chart is presented depicting ocean and atmosphere coupling. Based on highly cited popular research, possible mechanisms for Canonic ENSO, Modoki ENSO and Canonic-Modoki ENSO are proposed. Initiated by solar decadal variability how mid-latitude jets and tropospheric circulations (Walker and Hadley circulation) are modulated and in turn, influence ENSO is discussed. Such flow chart will help to improve our understanding of different types of ENSO in temporal as well as spatial scale. It will also benefit the modelling group to improve the representation of the ENSO in models.

The subsequent teleconnections by ENSO (for e.g.,) on ISM is also presented. Focusing on later two decades of the last century, how such connection could have been disrupted is analysed. During that period, the role of explosive volcanos and that of the sun both triggered positive phase of the NAO, which could be one important factor for possible disruption. Positive NAO via triggering Rossby wave around mid-latitudes could influence north Pacific and subsequently has the potential to modulate CP ENSO phase through the pathway of the atmospheric and oceanic bridge. It is also observed that there is a significant rising trend for CP ENSO, NAO and SLP around Darwin of Australia. The overall study also addresses how local N-S Hadley circulation, as manifests as NAO in the NH and IOD in the SH could have played a role in modulating ISM in later decades of the twentieth century. Interestingly, such observation is missed by models. This study also offers some explanation for few contradictory findings.

5. References.

Adams, J. B. Mann M. E. and Ammann C. M. et. al. (2003), Proxy evidence for an El Niño-like response to volcanic forcing, *Nature*, 426, 274-278, doi:10.1038/nature02101.

Allan, R. and Ansell, T., A new globally complete monthly historical gridded mean sea level pressure dataset (HadSLP2): 1850-2004, *J. Climate*, 19(22), 5816-5842, (2006).

Amita, P., Kripalani RH, Preethi, B and Pandithurai, (2016) Potential role of the February–March Southern Annular Mode on the Indian summer monsoon rainfall: a new perspective. *Climate Dynamics*. 47, 3-4, 1161-1179, DOI: 10.1007/s00382-015-2894-5.

Annamalai, Hanna, Kevin Hamilton, and Keneth R. Sperber.(2007), The South Asian summer monsoon and its relationship with ENSO in the IPCC AR4 simulations. *Journal of Climate* 20, 6, 1071-1092.

Annamalai, H, J Hafner, K. P. Sooraj, and P. Pillai, (2013), Global Warming Shifts the Monsoon Circulation, Drying South Asia, *J. of Clim.*, 26, 2701-2718.

Ashok K, Behera SK, Rao SA, Weng H, Yamagata T, El Niño Modoki and its possible teleconnections. *J Geophys Res* 112:C11007. doi:10.1029/2006JC003798, (2007).

Ashok K, Tam CY, Lee WJ. ENSO Modoki impact on the Southern Hemisphere storm track activity during extended austral winter. *Geophysical Research Letter* 36: L12705, DOI: 10.1029/2009GL038847, (2009).

Ashok, K., Guan, Z. and Yamagata, T., Impact of Indian Ocean Dipole on the Relationship between the Indian Monsoon Rainfall and ENSO. *Geo. Res. Lett.* 28, 23, 4499-4502, (2001).

Ashok, K and Yamagata T, Climate change: The El Niño with a difference *Nature* 461, 481-484. doi:10.1038/461481a, (2009).

Ashrit RG, Rupa Kumar K, Krishna Kumar K. ENSO-monsoon relationships in a greenhouse warming scenario. *Geophysical Research Letters* 28(9): 1727–1730, (2001).

Baldwin, M.P. and Dunkerton, T.J., Stratospheric harbingers of anomalous weather regimes. *Science*, 294, 5542, 581–584, DOI: 10.1126/science.1063315, (2001).

Bjerknes, J., A possible response of the atmospheric Hadley circulation to equatorial anomalies of ocean temperature, *Tellus*, 18, 4, 820–829, DOI: 10.1111/j.2153-3490.1966.tb00303, (1966).

Bollasina, M.A, et al. (2011), Anthropogenic Aerosols and the Weakening of the South Asian Summer Monsoon, *Science*, 334, 6055, 502-505, DOI: 10.1126/science.1204994.

Brönnimann, S., Ewen, T., Griesser, T., and Jenne, R., Multidecadal signal of solar variability in the upper troposphere during the 20th century, *Space Sci. Rev.*, 125(1-4), 305-317, 305-317, doi: 10.1007/s11214-006-9065-2, (2006).

Brown JN, McIntosh PC, Pook MJ, Risbey JS., An investigation of the links between ENSO flavors and rainfall processes in Southeastern Australia. *Monthly Weather Review* 137: 3786–3795, (2009).

Cai W, Cowan T., La Niña Modoki impacts Australia autumn rainfall variability. *Geophysical Research Letter* 36: L12805, DOI: 2009GL037885, (2009).

Cash, Benjamin A., et al. "Sampling variability and the changing ENSO–monsoon relationship." *Climate Dynamics*, 48, 11, 4071-4079, (2017).

Camp, C.D. et al., Stratospheric polar warming by ENSO in winter: A statistical study, *Geophys. Res. Lett.*, 34, L04809, doi: 10.1029/2006GL028521, (2007).

Carvalho L.M.V., Jones, C and Ambrizzi, T., Opposite phases of the Antarctic Oscillation and relationships with intraseasonal to interannual activity in the tropics during the austral summer, *J. of Clim.*, 18, 702-718, DOI: 10.1175/JCLI-3284.1, (2005).

Chang, C. P., P. Harr, and J. Ju, Possible roles of Atlantic circulations on the weakening Indian monsoon rainfall-ENSO relationship. *J. Climate*, 14, 2376-2380, (2001).

Chang CWJ, Hsu HH, Sheu WJ., Interannual mode of sea level in South China Sea and the roles of El Niño Modoki. *Geophysical Research Letter* 35: L03601, DOI: 10.1029/2007GL032562, (2008).

Chen, D., Cane, M. A., Kaplan, A., Zebiak, S. E. & Huang, D. J. Predictability of El Niño over the past 148 years. *Nature* 428, 733–736 (2004).

Christoforou, P. and Hameed, S., Solar cycle and the Pacific 'centers of action', *Geophys. Res. Lett.*, 24(3), 293-296, DOI: 10.1029/97GL00017, (1997).

Chung, C. E. and V. Ramanathan, Weakening of the North Indian SST gradients and the monsoon rainfall in India and the Sahel, *J. Clim.* 19, 2036, (2006).

Emile-Geay J., R. Seager, M.A. Cane, E. R. Cook, and G.H. Haug, (2008): Volcanoes and ENSO over the Past Millennium. *J. Climate*, 21, 3134-3148.

Frame, T.H.A. and Gray, L.J., The 11-year solar cycle in ERA-40 data: an update to 2008, *J. Climate*, Early online release, DOI: 10.1175/2009JCLI3150.1, (2009).

García-Herrera R, Calvo N, García RR, Giorgetta MA, Propagation of ENSO temperature signals into the middle atmosphere: a comparison of two general circulation models and ERA-40 reanalysis data. *J Geophys Res* 111:D06101. doi:10. 1029/2005JD006061, (2006).

Gill A. E., Some simple solutions of heat induced tropical circulations. *Q J R Meteorol. Soc* 106: 447-462, (1980).

Goswami, B.N., V. Venugopal, D. Sengupta, M. S. Madhusoodanan, P. K. Xavier, Increasing Trend of Extreme Rain Events Over India in a Warming Environment, *Science* 314, 1442, (2006).

Graf, H.-F., and D. Zanchettin (2012), Central Pacific El Niño, the “subtropical bridge,” and Eurasian climate, *J. Geophys. Res.*, 117, D01102, doi:10.1029/2011JD016493.

Gray, L.J., J. Beer and M. Geller, et al. (2010), Solar influences on climate. *Rev. Geophys.*, 48, RG4001, doi: 10.1029/2009RG000282.

Haigh, J. D., Blackburn, M., and Day, R., The response of tropospheric circulation to perturbations in lower-stratospheric temperature, *J. Climate*, 18(17), 3672-3685, (2005).

Haigh, J. D., The impact of solar variability on climate, *Science*, 272(5264), 981-984, (1996).

Haigh, J. D., A GCM study of climate change in response to the 11-year solar cycle, *Q. J. Roy. Meteor. Soc.*, 125(555), 871-892, (1999).

Haigh, J.D. and Roscoe, H.K., Solar influences on polar modes of variability, *Meteorol. Z.*, 15, 3, 371–378, doi: 10.1127/0941-2948/2006/0123, (2006).

Haigh, J. D., The effects of solar variability on the Earth's climate, *Philos. T. R. Soc. A.*, 361(1802), 95-111, (2003).

Ham, Y.-Y.; Kug, J.-S.; Park, J. Y.; Jin, F.-F. (2013a): Sea surface temperature in the north tropical Atlantic as a trigger for El Niño /Southern Oscillation events. *Nat. Geosci.*, 6, doi:10. 1038/NGEO1686.

Ham, Y.-Y., Kug, J.-S.; Park, J. Y.; Jin, F.-F. (2013b): Two distinct roles of Atlantic SSTs in ENSO variability: North tropical Atlantic SST and Atlantic Niño. *Geophys. Res. Lett.* , 40, 4012–4017.

Harrison, D.E. and Larkin, N.K. Darwin sea level pressure, 1876–1996: Evidence for climate change? *Geophysical Research Letters* 24: doi: 10.1029/97GL01789. issn: 0094-8276, (1997).

Held and Soden, Robust Responses of the Hydrological Cycle to Global Warming. *Journal of Climate*. 19, 5686-5699, (2006).

Hill, K. J, A. S. Taschetto, and M. H. England, South American rainfall impacts associated with inter-El Niño variations, *Geophysical Research Letters*, 36, L19702, doi: 10.1029/2009GL040164, (2009).

Huang, P. *et al.* *Patterns of the seasonal response of tropical rainfall to global warming. Nature Geosci.* 6, 357–361 (2013).

Hurwitz MM, Newman PA, Oman LD, Molod AM, Response of the Antarctic stratosphere to two types of El Niño events. *J Atm Sci* 68:812–822. doi:10.1175/2011JAS3606.1, (2011).

Hurrell et al., Influence of variations in extratropical wintertime teleconnections on northern hemisphere temperature, *Geophysical Research Letter*, DOI: 10.1029/96GL00459, (1996).

IPCC, 2013: Climate Change, The Physical Science Basis. Contribution of Working Group I to the Fifth Assessment Report of the Intergovernmental Panel on Climate Change, Cambridge University Press, Cambridge, United Kingdom and New York, NY, USA, 1535 pp, doi: 10.1017/CBO9781107415324, (2013).

Jones, P.D. Jonsson, T and Wheeler, D, Extension of the North Atlantic Oscillation using early instrumental pressure observations from Gibraltar and southwest Iceland, *Int. J. Climatol.* 17:1433-1450, (1997).

Kao H-Y, Yu J-Y., Contrasting eastern-Pacific and central-Pacific types of El Nino. *Journal of Climate*, 22: 615 – 632, (2009).

Kaplan, A., Cane M., Kushnir Y., Clement A., Blumenthal M., and Rajagopalan B., Analyses of global sea surface temperature 1856-1991, *J. of Geophys. Res.*, 103, 18,567-18,589, (1998).

Kendall, M. G., Rank Correlation Methods, 4th ed. London: Griffin, (1970).

Kistler, R., Collins, W., Saha, S., White, G., Woollen, J., Kalnay, E., Chelliah, M., Ebisuzaki, W., Kanamitsu, M., Kousky, V., van den Dool, H., Jenne, R., Fiorino, M., The NCEP-NCAR

50-year reanalysis: monthly means, CD-ROM and documentation. *Bull. Am. Meteorol. Soc.* 82, 247–267, (2001). Kodera, K. and Kuroda, Y., Dynamical response to the solar cycle. *J. Geophys. Res.*, 107, D24, 4749, doi:10.1029/2002JD002224, (2002).

Kripalani RH and A Kulkarni, Climate impact of El Nino / La Nina on the Indian Monsoon: A new perspective, *Weather*, 52, 39-46, (1997).

Kug J-S, Jin F-F, An S-I, Two types of El Niño events: cold tongue El Niño and warm pool El Niño. *J Climate* 22:1499–1515, (2009).

Kumar KK, Rajagopalan B, Cane MA, On the weakening relationship between the Indian Monsoon and ENSO. *Science* 284 (5423): 2156-2159, (1999).

Larkin NK, Harrison DE., On the definition of El Niño and associated seasonal average U.S. weather anomalies. *Geophysical Research Letters*, 32, L13705, DOI: 10.1029/2005GL022738, (2005).

Lean, J. and Rind, D., Earth's response to a variable Sun, *Science*, 292, 5515, 234-236, (2001).

Lee, J.N., D.T. Shindell, and S. Hameed, The influence of solar forcing on tropical circulation. *J. Climate*, 22, 5870-5885, doi:10.1175/2009JCLI2670.1, (2009).

Liu, X., and M. Yanai, Relationship between the Indian monsoon rainfall and the tropospheric temperature over the Eurasian continent. *Quart. J. Roy. Meteor. Soc.*, 127, 909-937, (2001).

Lorenzo E.D., K. M. Cobb, J. C. Furtado et al., Central Pacific El Niño and decadal climate change in the North Pacific Ocean, *Nature GeoScience*, 1-4, DOI: 10.1038/NGEO984, (2010).

Maity, R. and Kumar D. N., Bayesian dynamic modelling for monthly Indian summer monsoon rainfall using El Niño–Southern Oscillation (ENSO) and Equatorial Indian Ocean Oscillation (EQUINOO). *J. Geophys. Res.* 111:D07104, (2006).

McPhaden MJ, Lee T, McClurg D., El Nino and its relationship to changing background conditions in the tropical Pacific Ocean. *Geophysical Research Letters*. 38: L15709, DOI: 10.1029/2011GL048275, (2011).

Manzini E, Giorgetta MA, Esch M, Kornblueh L, Roeckner E, The influence of sea surface temperatures on the Northern winter stratosphere: ensemble simulations with the MAECHAM5 model. *J Climate* 19:3863–3881, (2006).

Mantua, N.J. and Hare, S. R. (2002): The Pacific Decadal Oscillation. *Journal of Oceanography*, 58, 1, 35-44.

McPhaden, M. J, and Zhang, D., Pacific Ocean circulation rebounds, *Geophys. Res. Lett.*, 31, L18301, doi:10.1029/2004GL020727, (2004).

Meehl, G. A., Arblaster, J.M., Branstator, G., and van Loon, H., A coupled air-sea response mechanism to solar forcing in the Pacific region, *J. Climate*, 21(12), 2883-2897, (2008).

Meehl, G. A., Arblaster, J. M., Matthes, K., Sassi, F., and van Loon, H., Amplifying the Pacific Climate System Response to a Small 11-Year Solar Cycle Forcing. *Science*, 325, 1114-1118, doi:10.1126/science.117287, (2009).

Miller J., D. R., Cayan, T. P. Barnett, N. E. Graham and J. M. Oberhuber , The 1976-77 climate shift of the Pacific Ocean. *Oceanography*, 7, 1, (1994). Myles Hollander and Douglas A. Wolfe, *Nonparametric Statistical Methods*, 2nd Edition, Wiley-Interscience, ISBN-10: 0471190454, ISBN-13: 978-0471190455, (1999).

Ohba M, H. Shiogama, T Yokohata and M Watanabe, (2013), Impact of Strong Tropical Volcanic Eruptions on ENSO Simulated in a Coupled GCM, *American Meteorological Society*, 26, 5169- 5182, DOI: 10.1175/JCLI-D-12-00471.1

Oliva et al. (2017), Recent Regional Climate Cooling on the Antarctic Peninsula and Associated impacts on the Cryosphere, *Science of the Total Environment*, 580, 210-223.

Polvani et al. (2017). The Impact of Ozone-Depleting Substances on Tropical Upwelling, as Revealed by the Absence of Lower-Stratospheric Cooling since the Late 1990s. *Journal of Climate*, 30, 2523, DOI: 10.1175/JCLI-D-16-0532.1.

Ramanathan, V. et al., Atmospheric brown clouds: Impacts on South Asian climate and hydrological cycle. *Proc. Natl. Acad. Sci. U.S.A.* 102, 15, 5326, (2005).

Randel WJ, Garcia R, Calvo N, Marsh D, ENSO influence on zonal mean temperature and ozone in the tropical lower stratosphere. *Geophys Res Lett* 36:L15822. doi:10.1029/2009GL039343, (2009).

Roxy et al. 2015, Drying of Indian subcontinent by rapid Indian Ocean warming and a weakening land-sea thermal gradient, *Nature Communications* 6, Article number: 7423, doi:10.1038/ncomms8423.

Roy, I. and Tedeschi, R. G., 'Influence of ENSO on regional ISM precipitation - local atmospheric Influences or remote influence from Pacific', *Atmosphere*, 7, 25; doi:10.3390/atmos7020025, (2016).

Roy, I. and Tedeschi, R. G. and Collins, M., 'ENSO teleconnections to the Indian summer monsoon in observations and models', *International Journal of Climatology*, 37,4, 1794-1813, DOI: 10.1002/joc.4811, (2017).

Roy and Collins, On identifying the role of Sun and the El Niño Southern Oscillation on Indian Summer Monsoon Rainfall, *Atmos. Sci. Let.*, 16: 162–169, DOI: 10.1002/asl2.547, (2015).

Roy, I. 'The role of the sun in atmosphere-ocean coupling' *International Journal of Climatology*, 34, 3, 655-677, doi:10.1002/joc.3713, (2014).

Roy, I. and Haigh, J. D., Solar cycle signals in sea level pressure and sea surface temperature, *Atmos. Chem. Phys.*, 10, 6, 3147–3153, (2010).

Roy, I. and Haigh, J.D., 'The influence of solar variability and the quasi-biennial oscillation on lower atmospheric temperatures and sea level pressure', *Atmospheric Chemistry and Physics* (ACP), 11, 11679-11687, ISSN:1680-7316. doi: 10.5194/acp-11-11679-2011, (2011).

Roy, I. and Haigh, J.D. Solar Cycle Signals in the Pacific and the Issue of Timings. *Journal of Atmospheric Science*, 69, 4, 1446-1451, doi: <http://dx.doi.org/10.1175/JAS-D-11-0277.1>, (2012).

Roy, I, T. Asikainen, V. Maliniemi, K. Mursula, 'Comparing the influence of sunspot activity and geomagnetic activity on winter surface climate', *Journal of Atmospheric and Solar-Terrestrial Physics*; doi:10.1016/j.jastp.2016.04.009, (2016).

Roy, I. The Role of Natural Factors on Major Climate Variability in Northern Winter. *Preprints*, 2016080025 (doi: 10.20944/preprints201608.0025.v1 (2016).

Sassi, F. et al., Effect of El Nino-Southern Oscillation on the dynamical, thermal, and chemical structure of the middle atmosphere, *J. Geophys. Res.*, 109, D17108, (2004).

Sato, M., Hansen, J. E., McCormick, M. P. and Pollack, J. B., Stratospheric aerosol optical depths (1850 – 1990), *J. Geophys. Res.*, 98, 22, 987–22, 994, (1993).

Schneider DP, Okumura Y, Deser C, Observed Antarctic interannual climate variability and tropical linkages. *J Climate*. 25:4048–4066. doi:10.1175/JCLI-D-11-00273.1, (2012).

Smith, T.M. and Reynolds, R. M., Improved extended reconstruction of SST (1854-1997). *J. Climate*, 17, 2466-2477, (2004).

Song H-J, Choi E, Lim G-H, Kim YH, Kug J-S, Yeh S-W, The central Pacific as the export region of the El Niño-Southern oscillation sea surface temperature anomaly to Antarctic sea ice. *J Geophys Res* 116:D21112. doi:10.1029/2011JD015645, (2011).

Stenchikov G, Delworth TL, Ramaswamy V, Stouffer, RJ, Wittenberg A and Zeng, F (2009), Volcanic signals in oceans, *J. of Geophysical Research*, 114, D16104, doi:10.1029/2008JD011673.

Sullivan A., Luo J.J. et al , Robust contribution of decadal anomalies to the frequency of central-Pacific El Niño. *Scientific Reports* 6(38540) DOI: 10.1038/srep38540, (2016).

Taguchi, M. and Hartmann, D.L., Increased occurrence of stratospheric sudden warmings during El Nino as simulated by WACCM, *J. Clim.*, 19, 324-332, (2006).

Taschetto AS, England MH., El Nino Modoki impacts on Australian rainfall. *Journal of Climate*, 22: 3167–3174, (2009).

Thompson, D.W.J. and Wallace, J. M. Annular modes in the extratropical circulation. Part I: month-to-month variability. *J. Clim.*, 13, 1000-1016, (2000).

Thompson et al., An abrupt drop in Northern Hemisphere sea surface temperature around 1970, *Nature*, 467, 444–447,(2010).

Trenberth, K.E. and Hoar T. J. The 1990-1995 El Niño-Southern Oscillation Event: Longest on record, *Geophysical Research Letters*, 23, 57-60, (1996).

Trenberth KE, Caron JM, Stepaniak DP, Worley S., Evolution of El Niño-Southern Oscillation and global atmospheric surface temperatures. *Journal of Geophysical Research* 107(D8): 4065, DOI: 10.1029/2000JD000298, (2002).

Vecchi, G.A. and Soden, B. J., Global Warming and the Weakening of the Tropical Circulation, *J. Climate.*, 20, 4316-4340, (2007).

Weng H, Behera SK, Yamagata T., Anomalous winter climate conditions in Pacific rim during recent El Niño Modoki and El Niño events. *Climate Dynamics* 32: 663–674, DOI: 10.1007/s00382-008-0394-6, (2009).

White, W. B., Lean, J, Cayan, D.R., and Dettinger, M.D., Response of global upper ocean temperature to changing solar irradiance, *J. Geophys. Res.-Oceans*, 102(C2), 3255-3266, (1997).

Xavier PK, Marzin C, Goswami BN (2007) An objective definition of the Indian summer monsoon season and a new perspective on the ENSO-monsoon relationship. *Q J R Meteorol Soc* 133:749–764

Yeh S, Kug J, Dewitte B, Kwon M, Kirtman B and Jin F, El Niño in a changing climate *Nature* 461, 511-4, (2009).

Yim, S Y, Bin Wang, Jian Liu, Zhiwei Wu, A comparison of regional monsoon variability using monsoon indices, *Clim Dyn*, 2013, DOI 10.1007/s00382-013-1956-9, (2013).

Yu J-Y., and H.-K. Kao, Decadal changes of ENSO persistence barrier in SST and ocean heat content indices: 1958-2001. *J. Geophys. Res.*, 112, D13106, doi:10.1029/ 2006JD007654, (2007).

Yu., J.-Y., H.-Y. Kao and T. Lee, Subtropics-Related Interannual Sea Surface Temperature Variability in the Equatorial Central Pacific. *Journal of Climate*, 23, 2869-2884, (2010).

Yu., J.-Y. and S. T. Kim, Relationships between Extratropical Sea Level Pressure Variations and the Central-Pacific and Eastern-Pacific Types of ENSO, *Journal of Climate*, 24, 708-720, (2011).

Yu and Kim, Identification of Central-Pacific and Eastern-Pacific types of ENSO in CMIP3 models, *Geophysical Research Letters*, 37, 15, 10.1029/2010GL044082, (2010).

Zhang, Y., Wallace, J. M. and Battisti, D. S., ENSO-like interdecadal variability: 1900–93. *J. Climate*, 10, 1004–1020, (1997).

Zhang, D. and McPhaden, M. J., Decadal variability of the shallow Pacific meridional overturning circulation: Relation to tropical sea surface temperatures in observations and climate change models. *Ocean Modelling*, 15, 3-4, 250-273, (2006).

Zhao, M. and Dirmeyer, P., Pattern and trend analysis of temperature in a set of seasonal ensemble simulations. *Geophys. Res. Lett.*, 30, doi: 10.1029/2003GL018579, (2003).

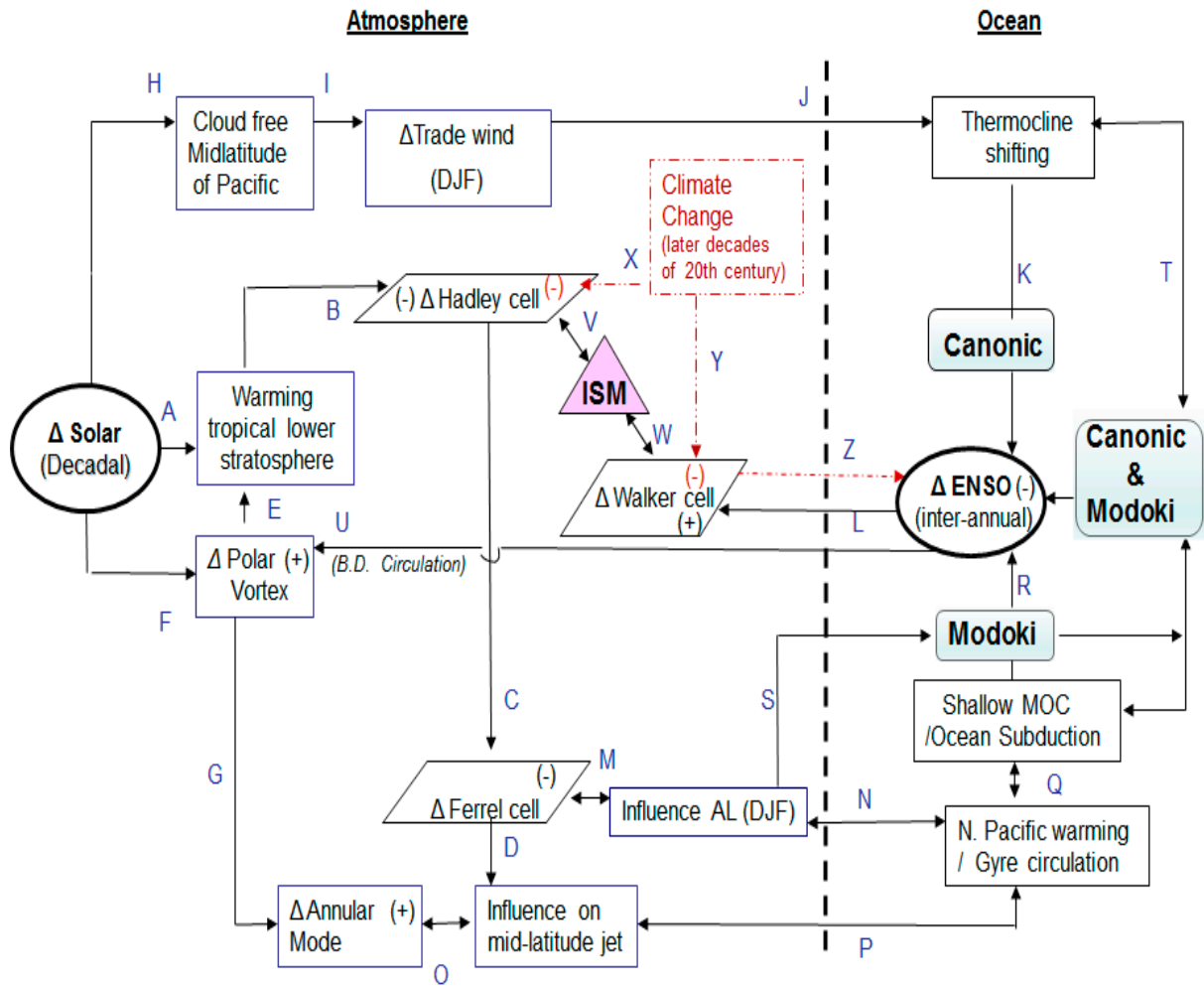
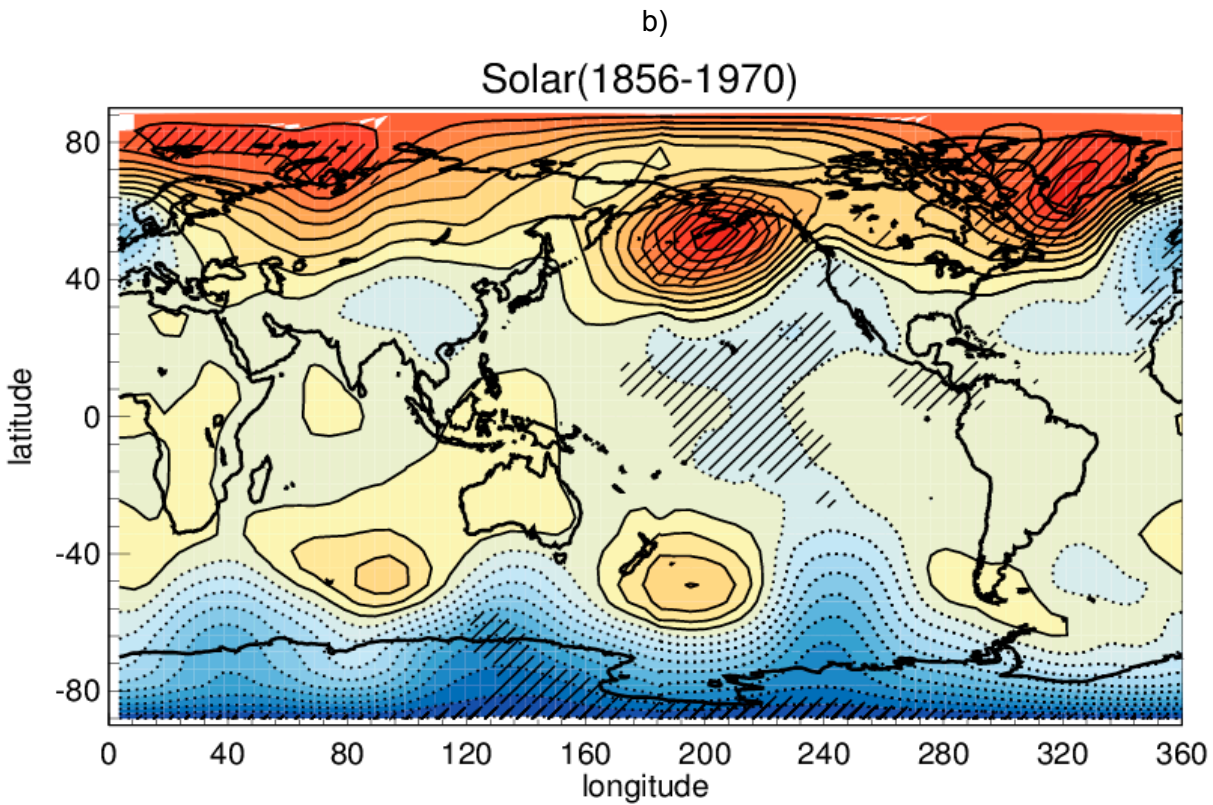
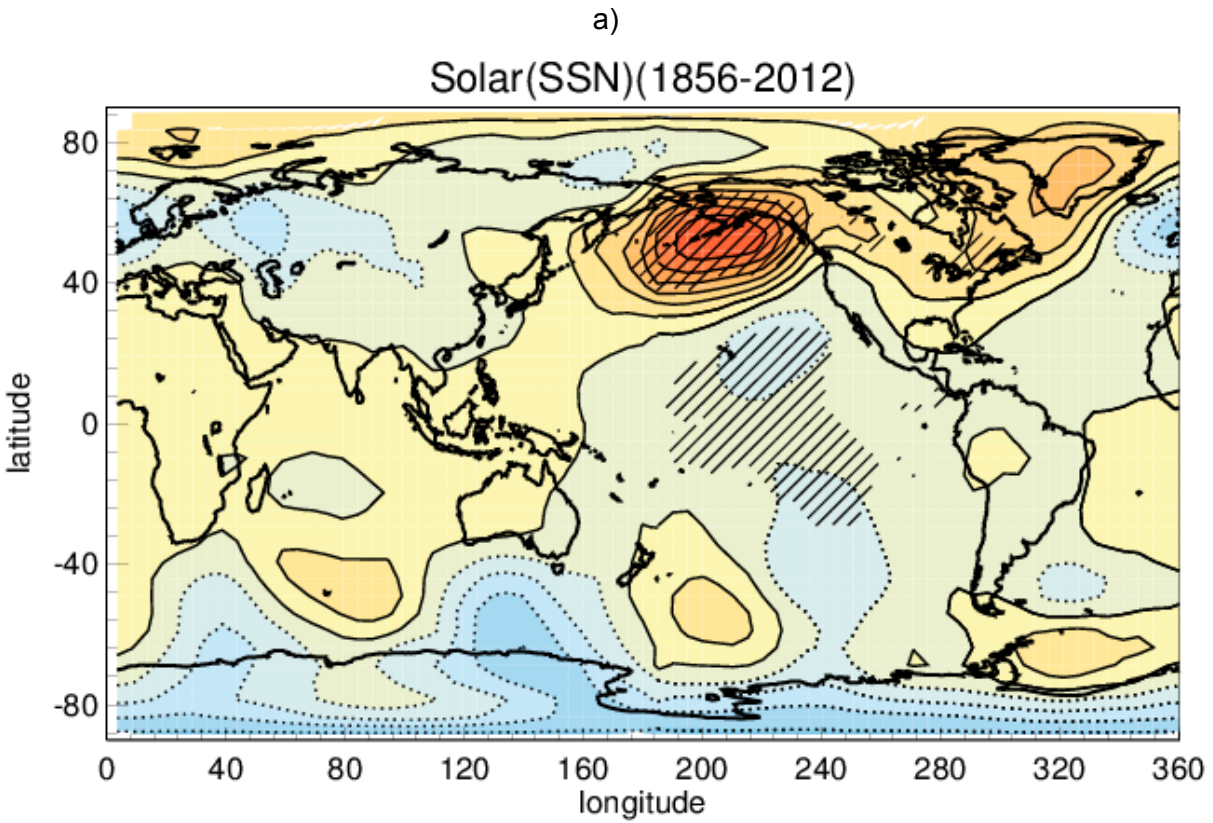


Fig.1. Flow chart showing the role of the sun in an atmosphere and ocean coupling mainly during DJF and the possible mechanism for Canonic ENSO, Modoki ENSO and Canonic-Modoki ENSO. ENSO-related teleconnection (e.g., ISM) affected by climate change period is shown by the dash-dotted line.



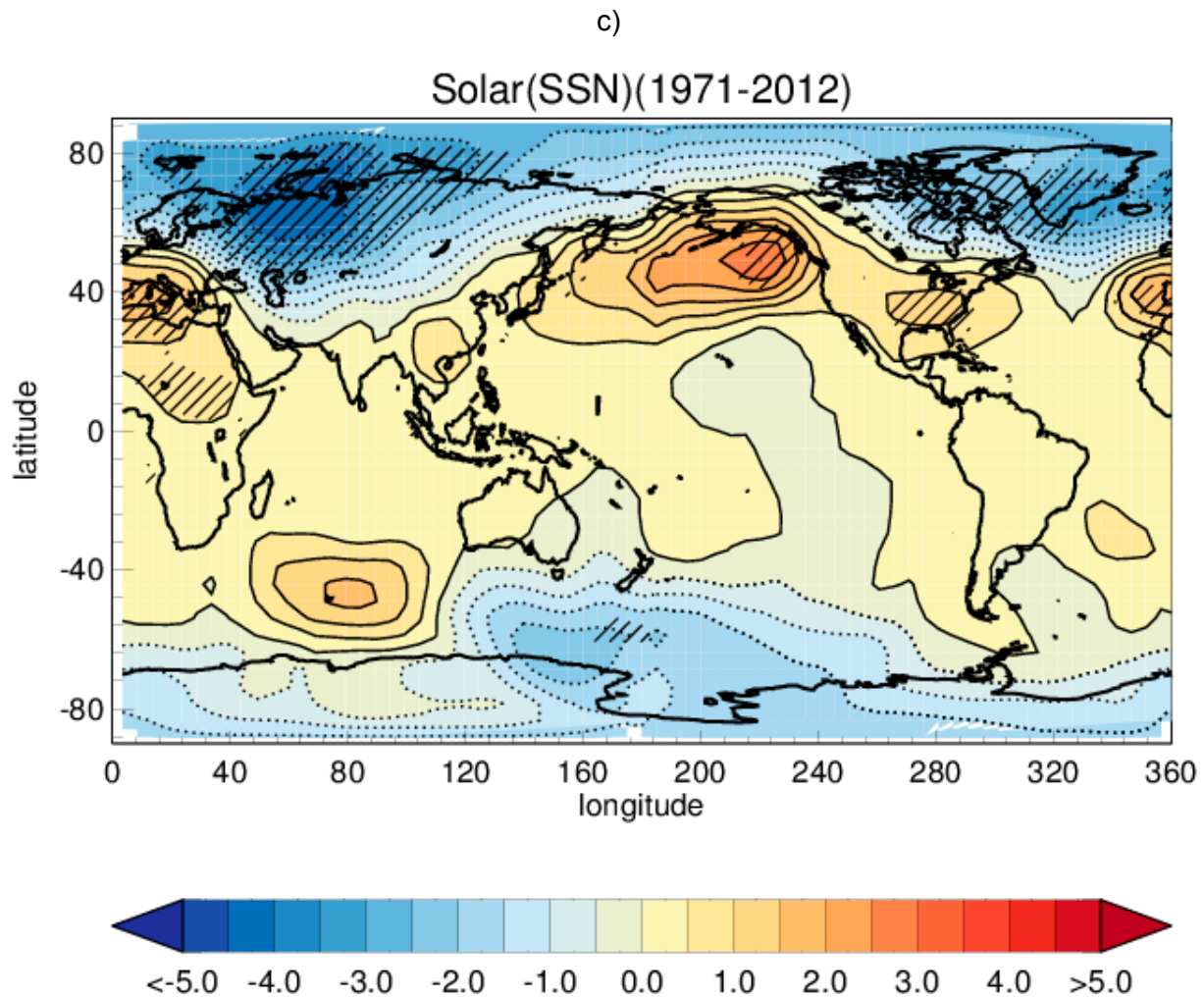


Fig. 2. The solar cycle signal (max-min, hPa) in DJF HADSLP2 data obtained from a multiple linear regression analysis using monthly SSN. Other indices used are ENSO, AOD (volcano) and trend. Different periods are used: (a) result for the entire period (1856-2012), b) for an earlier period (1856-1970) and (c) a latter period (1971-2012). Significant regions at the 95% level using a two-sided Student's t-test are shaded and dotted lines indicate negative contours.

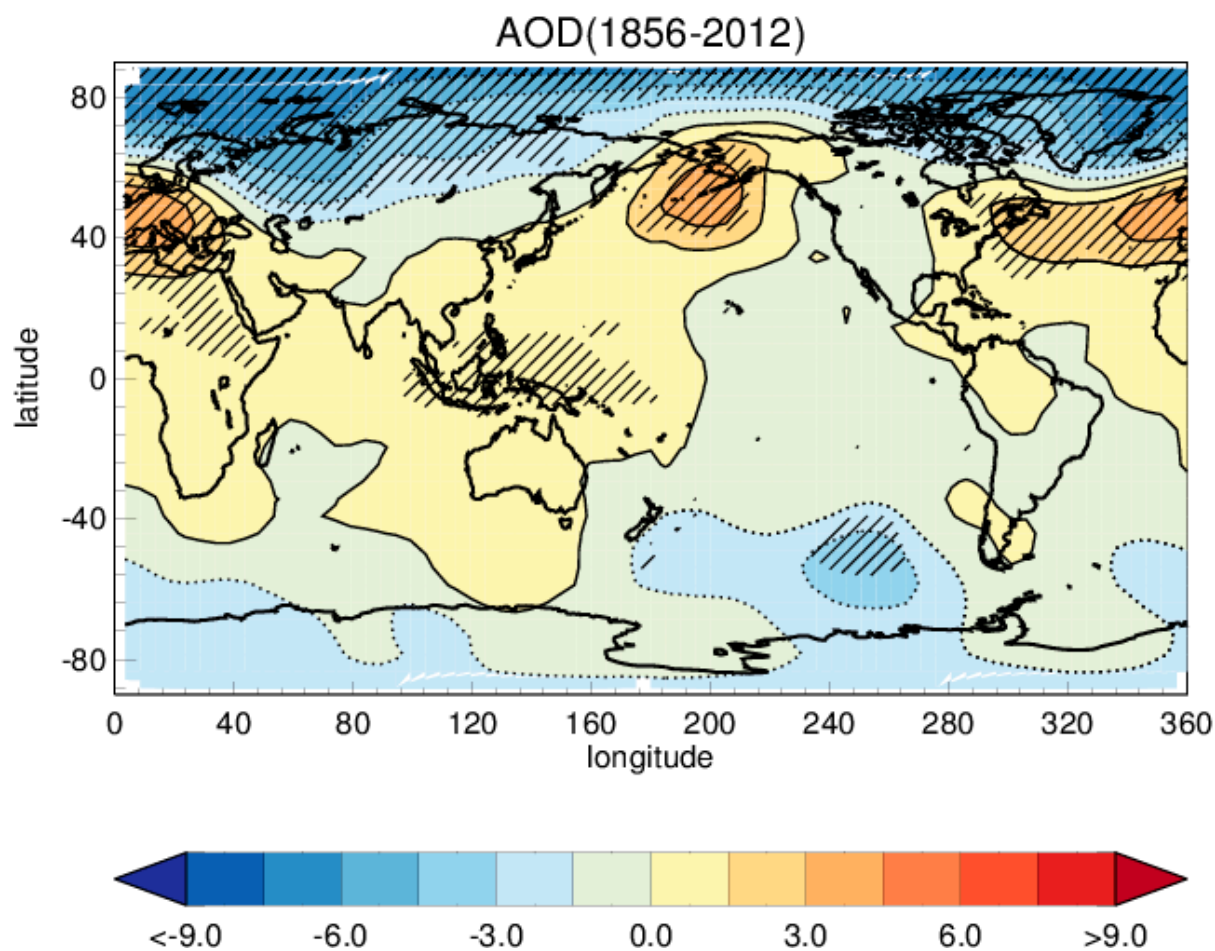
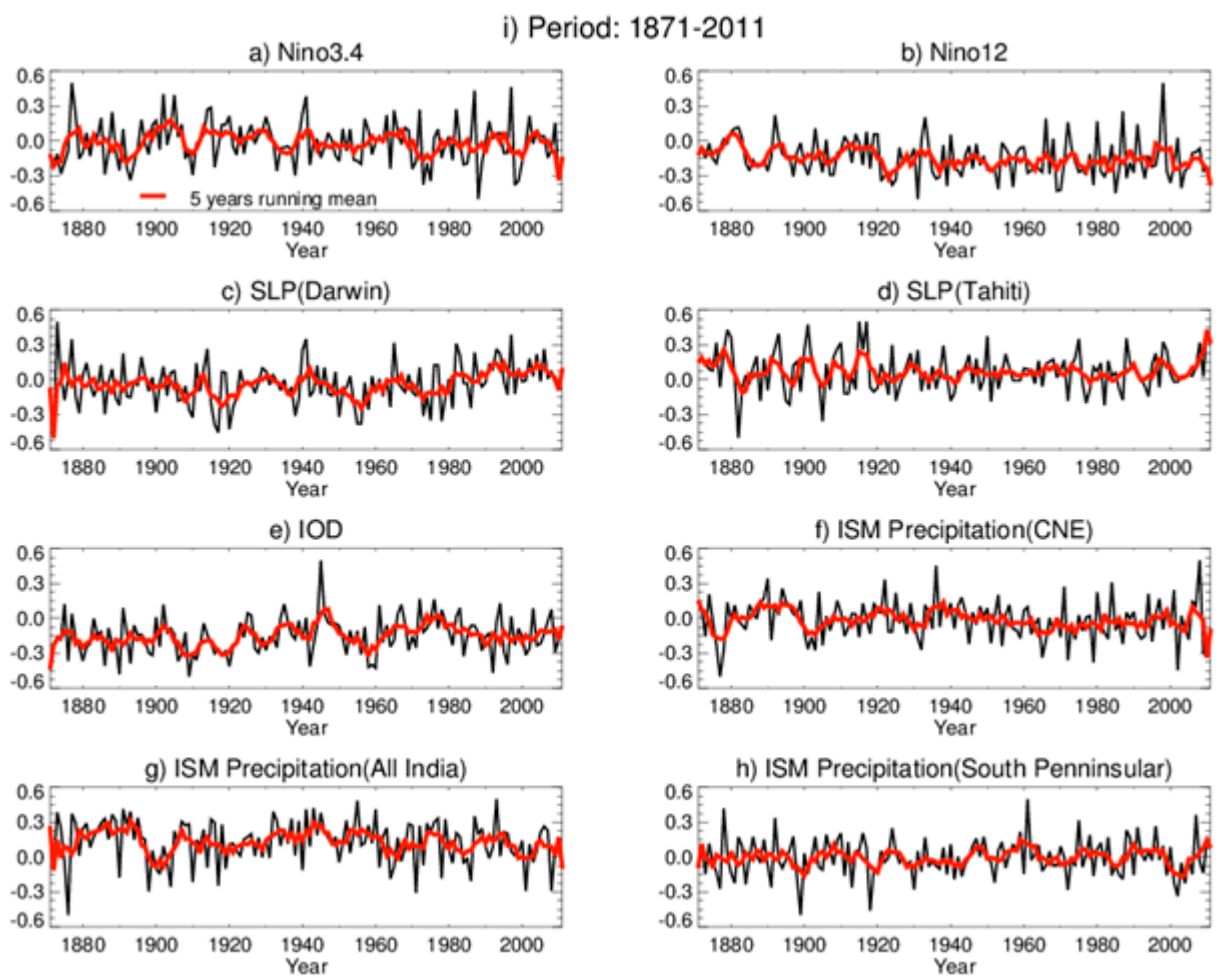


Fig. 3. Same as Fig 2a but it presents the signal due to the volcano (AOD).



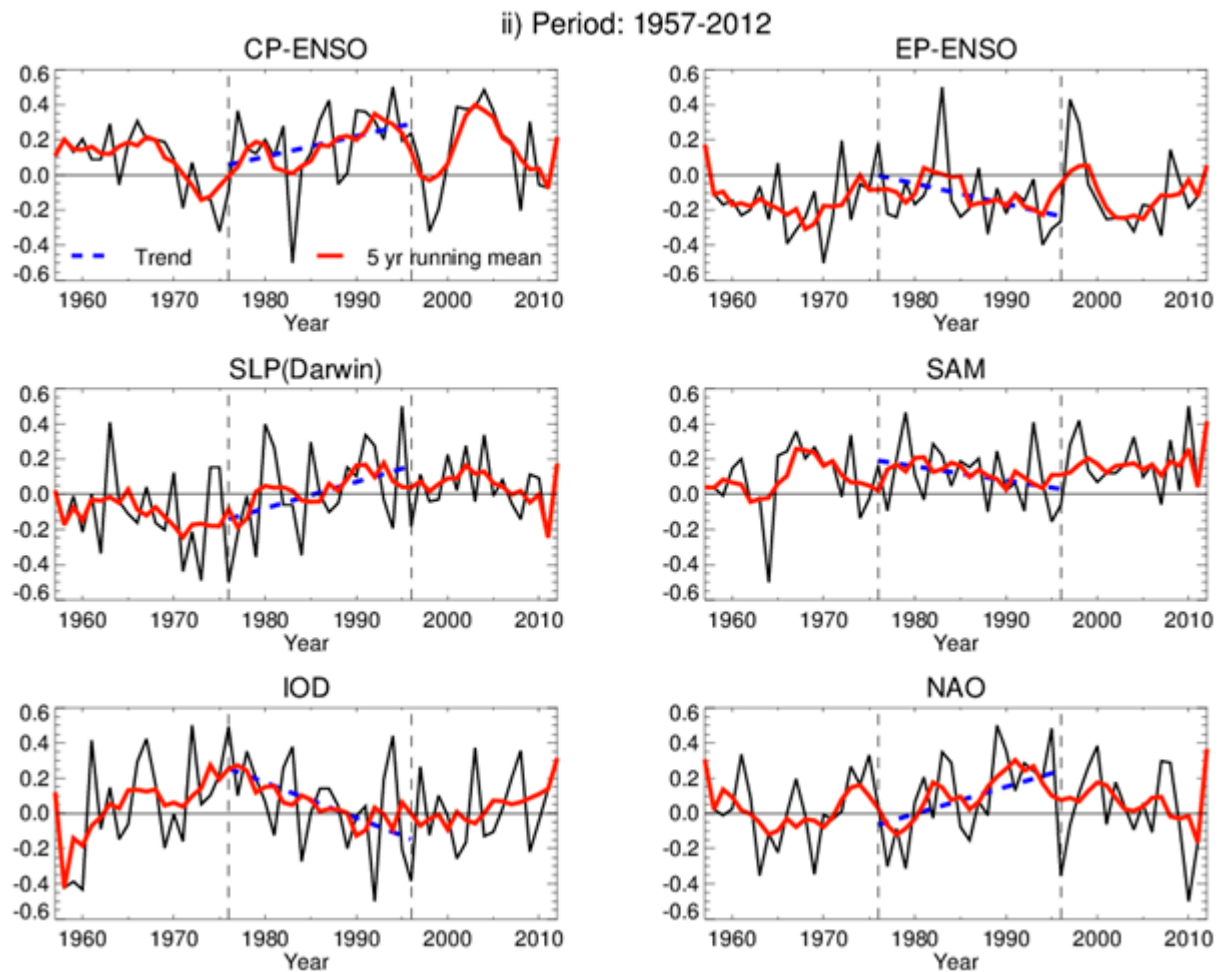


Fig.4. Normalised time series of various seasonal modes of climate variability i) during the period 1871-2011 (top panel) and ii) period 1957-2012 (bottom panel). For all cases, JJA value is considered, while for NAO, it is DJF. Five-year running mean of each series is marked by red in each panel. A trend line is plotted during 1976-1996 for all series of bottom panel and shown by a blue dashed line. Black dash lines demarcate the time period of 1976-1996.

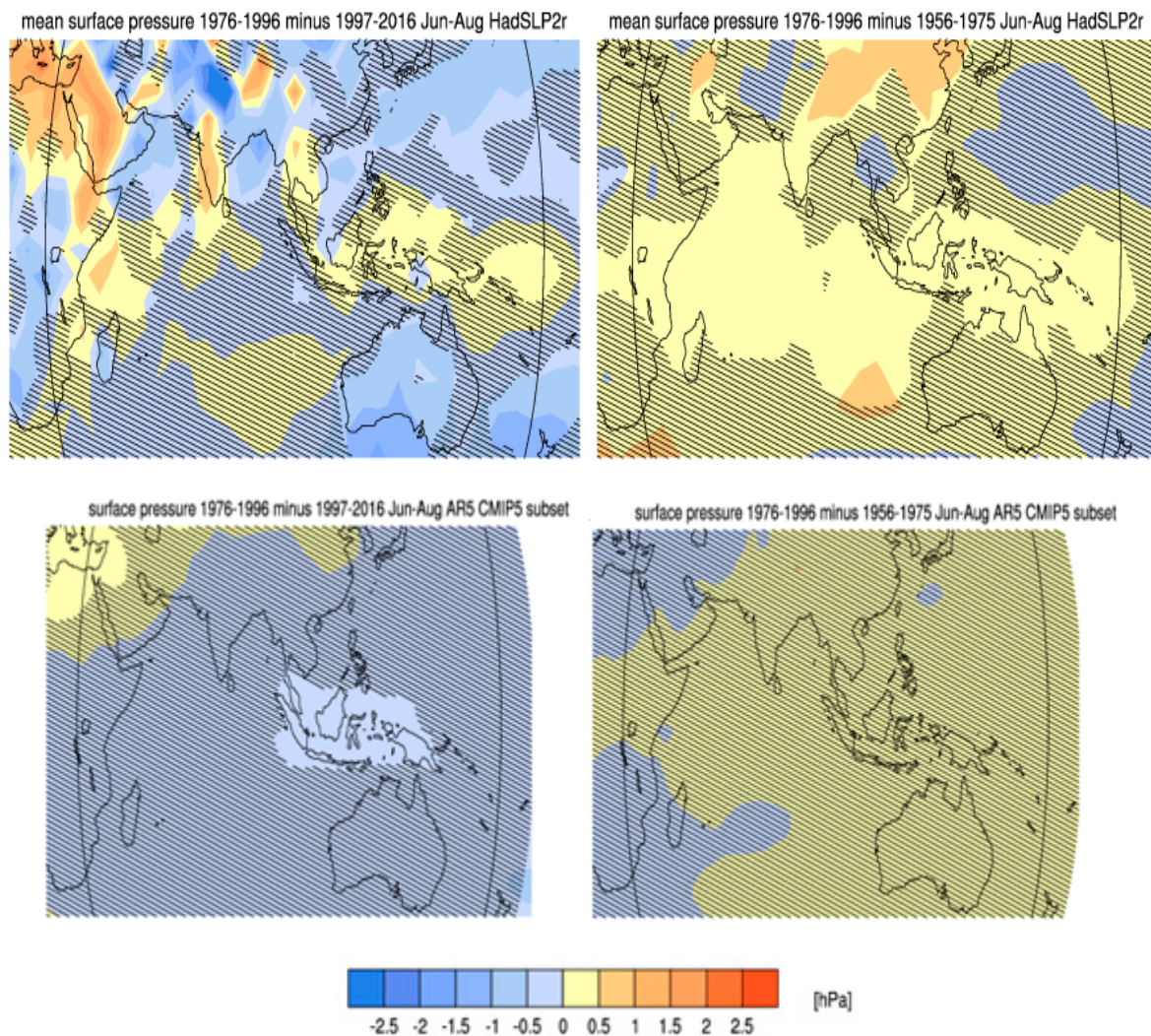


Fig.5. Mean surface pressure (June-Aug): 1976-1996 minus 1956-1975 (Right); 1976-1996 minus 1997-2016 (Left). The top panel shows observational data from HadSLP2r, while the bottom panel uses ensemble mean of GCM, CMIP5 (IPCC AR5) subset model. The signal smaller than one standard deviation of natural variability is shown by hatching. Plots generated using the IPCC's Climate Change Atlas, climexp.knmi.nl/plot_atlas_form.py.

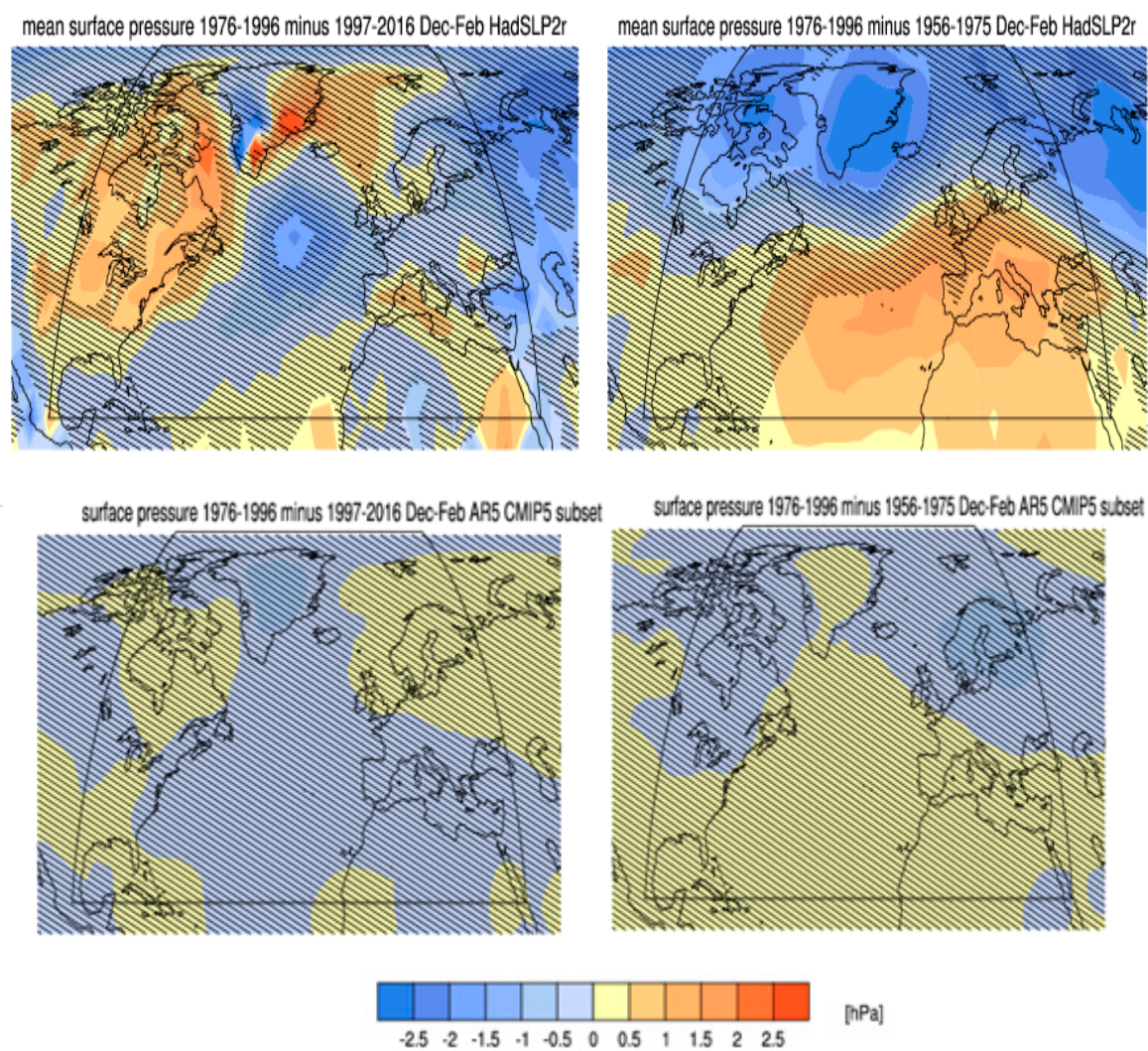


Fig.6. Same as Fig. 5 but mean surface pressure is for Dec-Feb with a particular focus on North Atlantic region.

Table -1: Indicate whether the pathways are evidenced or hypothesised.

	Observation	Mechanism	
		Explained	Hypothesised
Lower Stratosphere (A-D,H,I,M)	A,B,C,D,H,I,M	A,B,C,D,I	H, M
Upper Stratosphere (E-G,O)	F,G	E, F,O	
Atmosphere-ocean Coupling (J-L,N,P-T,U-W)	J, K, L, U, S, P	J,K,L,N,T,V,W,Q	N,P,Q,R,S
Climate Change (X-Z)	X, Y, Z	Z	

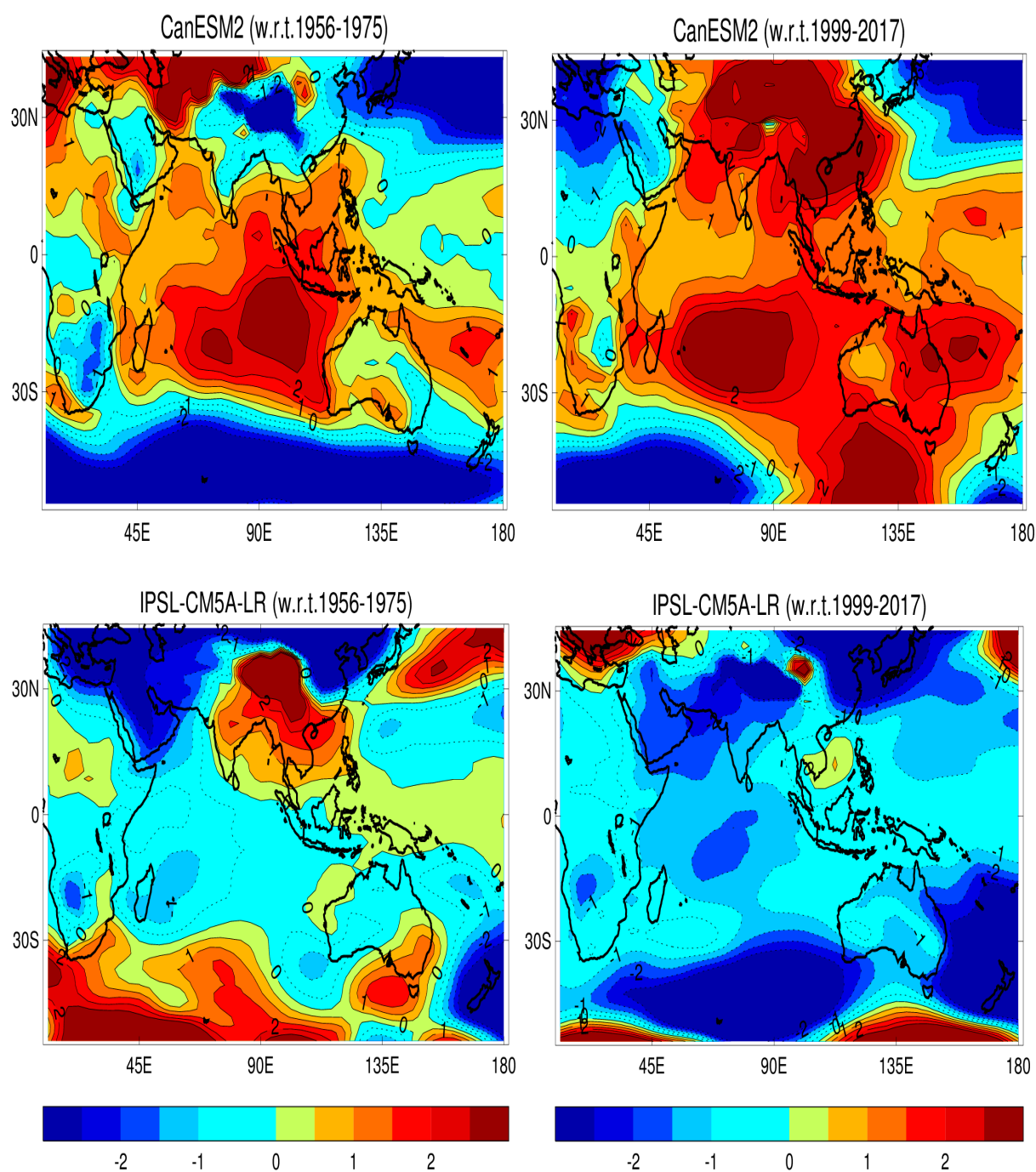


Fig.S1. Mean surface pressure (June-Aug): 1976-1996 minus 1956-1975 (Left); 1976-1996 minus 1997-2016 (Right) for two arbitrarily chosen CMIP5 models, CanESM2 (top) and IPSL-CM5A-LR (bottom).